University of Alberta

PRACTICAL ISSUES IN CONTROLLER PERFORMANCE MONITORING

by

Mridul Jain 

A thesis submitted to the Faculty of Graduate Studies and Research in partial fulfillment of the requirements for the degree of **Master of Science**.

in

Process Control

Department of Chemical and Materials Engineering

Edmonton, Alberta
Fall 2006

Your file Votre référence
ISBN: 978-0-494-22291-1
Our file Notre référence
ISBN: 978-0-494-22291-1

Abstract

Controller performance monitoring forms the backbone of any automation system and hence an integral part of process control software. This work deals with some practical issues relating to computation of performance monitoring tools. A method is devised to automatically detect Integrated White Noise (IWN) type disturbance in a system and compute a performance metric for such cases. A performance metric to measure the set-point tracking performance of a controller is also defined.

The conventional performance indices give a good estimate of the controller performance, but fail to tell the benefits of improving the performance. A methodology is developed to integrate controller performance and the economic impact of improving the performance via the Economic Performance Index (EPI).

Presence of stiction in control valve induces oscillations in the system and cause poor performance. A novel method to quantify stiction using a two-parameter stiction model also is presented in this work.

Acknowledgements

I am grateful to the many people who have contributed to the work described in this thesis. This is a difficult task, given the large number of people that have helped to design, implement, apply, criticize, sponsor and evangelize the work. I am going to try anyway, and if your name is not listed, rest assured that my gratitude is no less than for those listed below.

The first person I would like to thank is my supervisor, Dr. Sirish Shah. He has been the driving force behind this work. He has been an excellent mentor and great inspiration for me. I admire him for the enthusiasm and the drive he has towards quality work. I also admire him for the amount of patience he has shown in handling my numerous questions. And it goes without saying, this work wouldn't have even started if it was not for Dr. Shah's excellent guidance and support. Thank you Dr. Shah.

The second in the list comes Dr. Shoukat Choudhury. He is a role model to me. I admire his excellent knowledge and always ready-to-learn-more attitude. The attention he pays towards details is remarkable and something that I hope rubs off onto me. I would like to thank him for all the time he has spent in discussing and solving the problems I faced.

A special thanks to Dr. Rohit Patwardhan from Matrikon Inc. and Dr. Ramesh Kadali from Suncor for their help and support during my projects at Matrikon and Suncor, respectively. I would also like to thank my group members, Sankar, Varma, Venkat, Saneej, Hailei, Enayet, Syed, Salim, Ian and Rumana for their support.

I also want to acknowledge the NSERC-Matrikon-Suncor-iCORE-IRC group for financial support and for giving me the opportunity to work on different projects. I want to thank Matrikon Inc. and Suncor for letting me use their resources and Suncor for the financial support during my stay in Fort McMurray.

A very special thanks to my family, my parents, my brother without whom there is no meaning to all this. Their support, encouragement, faith and love cannot be substituted. A special thanks to Sapna for tolerating me and my unpredictable mood through the the two years and still giving me that support. Thanks to my roommates Hemant, Japan and Ashish for the delicious food and all my friends, Mranal, Ritika, Aashima, Sankar, Varma, Hari, Venkat, Saneej and Karteek for showing that you can work and yet have fun as a graduate student.

Mridul Jain
September 2006

Contents

List of Tables

List of Figures

List of Symbols

EPI	Economic Performance Index
IWN	Integrated White Noise
J	Slip-jump
$LFAR$	Low Frequency Amplitude Ratio
MVC	Minimum Variance Control
mv	Valve Output
op	Controller Output
pv	Process Output
PI	Performance Index
RPI	Relative Performance Index based on normal process data
RPI'	Relative Performance Index based on differenced data
RPI_{servo}	Relative Performance Index for set-point tracking
S	Deadband + Stickband

1 Introduction

The concept of Control Performance Monitoring and Assessment is well defined and it's importance is clearly stated in a recent work by Jelali (2006).*"Control performance monitoring / assessment (CPM/ CPA) is an important asset-management technology to maintain highly efficient operation performance of automation systems in production plants. The term monitoring means the action of watching out for changes in a statistic that reflects the control performance over time. The term assessment refers to the action of evaluating a statistic that reflects control performance at a certain point in time".* This study presents different aspects of control performance monitoring and assessment. Performance assessment is examined from two different perspectives;as a conventional performance metric and from an economic point of view, i.e. the economic impact of improved performance monitoring. The second part of this study focuses on the diagnosis aspect of performance monitoring. In particular, the common cause of oscillations in closed loop systems, detection and quantification of valve stiction, which cause poor performance.

1.1 Performance Monitoring and Assessment

In a typical continuous process industry, there are thousands of control loops. Keeping track of the performance of each and every loop is an

uphill task. It is known that 60% of the control loops have performance problem (Bialkowski (1993), Ender (1993), Rinchart and Jury (1997)). The various performance assessment tools developed over the last decade and a half provide a good measure of the controller performance. The most notable work is by Harris (1989) who applied time-series analysis to find the controller invariant term from routine operating data and used it as a benchmark to assess the closed-loop performance. This benchmark, known as the Minimum Variance Control (MVC) benchmark, provides the lower bound of process variance (hence upper bound for controller performance). The corresponding performance index is known as the Harris Index. Huang *et al.* (1997) and Huang and Shah (1999) later developed an efficient, stable filtering and correlation ($FCOR$) method to estimate this MVC benchmark and extended this to the multivariate case

Desborough and Harris (1993); Stanfelj *et al.* (1993) and Huang *et al.* (2000) also extended the MVC benchmarking concept to feedback / feedforward control loops. Tyler and Morari (1995); Tyler and Morari (1996) and Lynch and Dumont (1996) modified the Harris Index and extended it to unstable and nonminimum-phase system. In the work by Harris *et al.* (1996), Huang *et al.* (1997), Huang and Shah (1998), Huang and Shah (1999), Ko and Edgar (2001), McNabb and Qin (2003) and McNabb and Qin (2005) the concept of Harris index has been applied to multi-input multi-output ($MIMO$) systems.

Although MVC is a very convenient performance assessment benchmark and can be calculated with minimum process knowledge (knowledge of Process time delay) and closed loop data, it is not a target that most of the industrial controllers try to achieve. This is because, MVC often generates large control moves which have undesirable effect on the actuator and may pose safety issues. Therefore, Harris Index also better known as the Performance Index (PI), based on the MVC benchmark is generally used as a good first stage assessment tool, i.e. feedback controllers that shows performance close to MVC (high PI) do not require further analysis, but controllers that perform poorly with respect to MVC benchmark need to be examined further although they may not necessarily be providing poor controller. To obtain a measure of the real or practical performance of such controllers a further analysis of the performance limitations and comparison to the more practical benchmarks is required.

The Relative Performance Index, RPI (Gao *et al.* (2003), Huang and Shah (1999)) which is based on user defined benchmarks is a more practical performance assessment tool. Details of RPI are given in chapter 2. Chapter 2 also discusses practical issues related to RPI calculations in presence of Integrated White Noise (IWN) type disturbance in the system. IWN as discussed in chapter 2 is commonly encountered in real systems; and it poses variability issues in RPI and solutions of these aspects are detailed in chapter 2.

Chapter 3 gives a brief introduction to the difference between, stochastic and deterministic performance monitoring. It also talks about shortcomings of presently used technique of calculating RPI for servo (set-point tracking) problems. A new method to calculate RPI for servo problems is presented therein..

1.2 Economics

Chapter 4 gives a different perspective to the problem of Controller Performance Monitoring. It provides a measure of economic impact and a new performance metric, titled Economic Performance Index (EPI) is introduced. In an industrial setting the final decisions are based on economics. Any project that gets a go-ahead has to first pass the economic test. This holds true for any projects related to Process Control or Advanced Process Control as well. There has been some work done in the past on economic benefit analysis of implementing Advanced Control Systems by Muske (2003) and Bauer and Craig (2006). This work presents a methodology to extend the idea of economic performance assessment to day-to-day performance monitoring of controllers. A performance index is developed which gives a dual measure of the controller performance: it's present performance and the economic benefits of improving the performance to some desired level.

1.3 Oscillations in control loop

The last part of this thesis deals with the diagnosis of poor controller performance and in particular the presence of non-linearities in control loops. The presence of a non-linearity in a control loop often leads to oscillations

in a control loop and hence poor performance. These non-linearities can be due to: (1) Valve non-linearity, due to stiction, deadband and hysteresis; (2) the presence of non-linear external oscillations, and/or (3) non-linearity in the process.

About 30% of the oscillations in control loops are due to valve problems (e.g. the presence of static friction or stiction). Therefore, detection and quantification of stiction in control valves is an important issue in the process industry. There are several stiction detection methods (Choudhury *et al.* (2004*c*), Choudhury *et al.* (2004*b*), Horch (1999), Singhal and Salsbury (2005), Stenman *et al.* (2003), Srinivasan *et al.* (2005*a*), Srinivasan *et al.* (2005*b*)) available . However quantifying stiction still remains a challenge. Choudhury *et al.* (2004*b*), Srinivasan *et al.* (2005*a*) and Srinivasan *et al.* (2005*b*) have tried to quantify stiction, but in all these methods stiction is modelled as a one-parameter model (the one-parameter stiction model proposed by Stenman *et al.* (2003), which is not the correct way to model stiction phenomenon. These issues are explored explained in more detail in chapter 5. A novel method to quantify stiction is also proposed in chapter 5.

Chapter 6 gives some concluding remarks about the entire study followed by suggestions on future work.

2

Relative Performance Index and Integrated White Noise

2.1 Relative Performance Index (RPI)

RPI, (Gao *et al.* (2003), Huang and Shah (1999)) based on a user-defined benchmark gives a more practical measure of process performance. The benchmark can be in terms of desired closed-loop dynamics, such as settling-time, overshoot, decay-ratio etc. or even a historical performance.

Settling time benchmark: Settling time for a controller is a time period over which the process variable returns to the set point after a disturbance. Performance measure with settling time as benchmark is a comparison of the actual settling time a controller takes to what is desired. This idea is widely used in single loop performance assessment. RPI_{stime} (Gao *et al.* (2003))is defined as

$$RPI_{stime} = \frac{\text{desired settling time performance}}{\text{actual settling time performace}} = \frac{(1 + {h_1}^2 + {h_2}^2 + ...)}{(1 + {g_1}^2 + {g_2}^2 + ...)} \quad (2.1)$$

where $g_1, g_2, ...$ are the closed loop impulse response coefficients calculated using the present data and $h_1, h_2, ...$ are the closed loop impulse response coefficients of the desired dynamics (with user-defined settling time). The

implied assumption here is the system is Linear Time Invariant (LTI). The computational aspect of estimating $h_i's$ and $g_i's$ are discussed in more detail in section 3.1. In this work RPI_{stime} is used as the performance indicator and henceforth is referred simply as RPI.

It is observed that in presence of Integrated White Noise (IWN) type disturbance, i.e. when the noise model is an integrator ($N = 1/s$), the RPI fluctuates, even if the controller tuning and the process model fidelity remain the same. This is clear from figure 2.1 which shows RPI of a system with IWN type disturbance, over 10 different data segments. High variation in RPI can be clearly noticed. This leaves a very uncertain picture about the actual controller performance and also hurts the credibility of the performance metric.

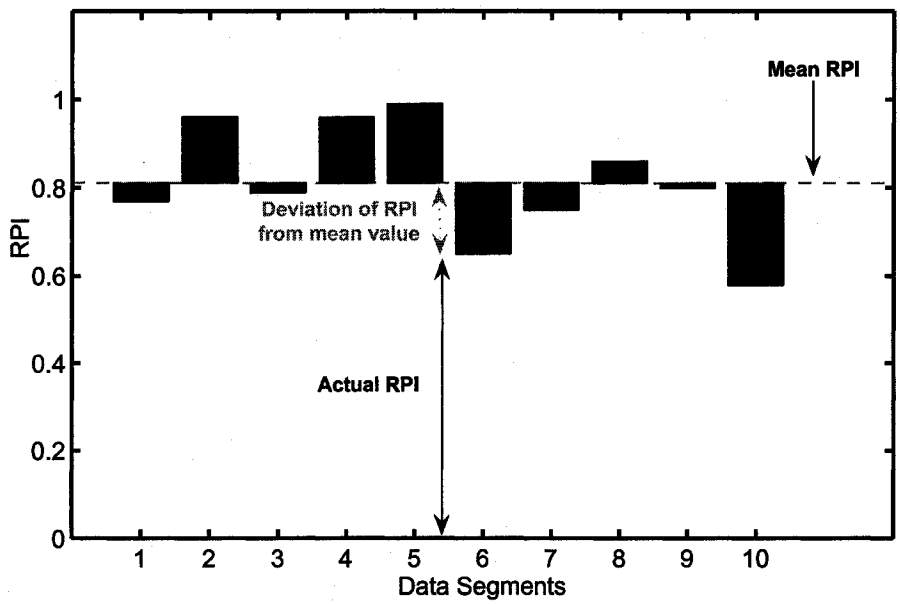

Figure 2.1: *RPI variation for a system with IWN type disturbance*

The fluctuating metric is a result of changing disturbance, but RPI does not differentiate between the changing disturbance model and controller tuning. Therefore the measure proposed in equation 2.1 does not correctly evaluate controller performance. In this chapter a method of computing RPI in presence of IWN type disturbance in suggested. This new metric is able to handle the problem of fluctuating disturbance. The

treatment of this problem is divided in two parts:

- Detecting the presence of IWN type disturbance in the system.
- Computing RPI for such cases.

The next section details a technique to detect IWN type disturbance in a closed loop system and a methodology for automatic detection is also presented.

2.2 Detecting Integrated White Noise (IWN) type disturbance

Consider a closed loop system shown in figure 2.2. The closed loop transfer function is given by

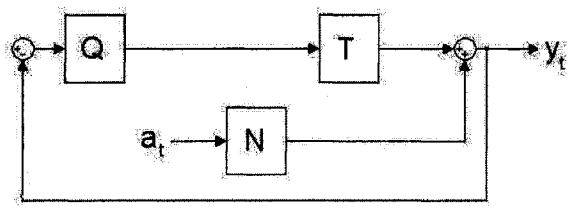

Figure 2.2: *A closed loop system*

$$y_t = \frac{TQ}{1+TQ} y_{sp} + \frac{N}{1+TQ} a_t \tag{2.2}$$

where N is the disturbance model, T is the process model and Q is the controller. If there is no set-point activity ($y_{sp} = 0$) then

$$y_t = \frac{N}{1+TQ} a_t \tag{2.3}$$

Consider a simple case when T and Q are given by

$$T = \frac{Ke^{-\theta s}}{(\tau s + 1)} \tag{2.4}$$

$$Q = K_c \left(1 + \frac{1}{\tau_I s}\right) \tag{2.5}$$

i.e. a PI controller. The closed loop transfer function (T_{cl}) for any noise model N can be written as

$$T_{cl} = \frac{N}{1 + K\left(\frac{e^{-\theta s}}{\tau s+1}\right) K_c \left(1 + \frac{1}{\tau_I s}\right)}$$

$$T_{cl} = \left(\frac{\tau_I s(\tau s + 1)}{(\tau s + 1)\tau_I s + KK_c e^{-\theta s}(\tau_I s + 1)}\right) N \tag{2.6}$$

Next consider two cases: one where the disturbance model N is an integrator, $N = 1/s$, i.e. a system with IWN type disturbance and second when $N = 1$, i.e. system with white noise type disturbance.

Case 1: $N = \frac{1}{s}$

$$T_{cl} = \left(\frac{\tau_I s(\tau s + 1)}{(\tau s + 1)\tau_I s + KK_c e^{-\theta s}(\tau_I s + 1)}\right) \frac{1}{s}$$

$$T_{cl} = \frac{\tau_I(\tau s + 1)}{(\tau s + 1)\tau_I s + KK_c e^{-\theta s}(\tau_I s + 1)} \tag{2.7}$$

The steady state response ($s = 0$) for this system is

$$T_{cl} = \frac{\tau_I}{KK_c} \tag{2.8}$$

Case 2: $N = 1$

$$T_{cl} = \frac{\tau_I s(\tau s + 1)}{(\tau s + 1)\tau_I s + KK_c e^{-\theta s}(\tau_I s + 1)} \tag{2.9}$$

The steady state response for this case is

$$T_{cl} = 0 \tag{2.10}$$

Thus in general, the steady state response of a system with IWN type disturbance is a non-zero value, while it tends to zero for a pure white noise type disturbance. Figure 2.3 shows this result via the frequency response curves for equations 2.7 and 2.9 for a process listed below. The plots are generated using $MATLAB$ with process model(T) and controller(Q) explicitly defined as

$$T = \frac{2e^{-10s}}{25s + 1} \tag{2.11}$$

$$Q = 0.83\left(1 + \frac{1}{25s}\right) \tag{2.12}$$

and noise model $N = 1/s$ or 1 for IWN or white noise type disturbance, respectively.

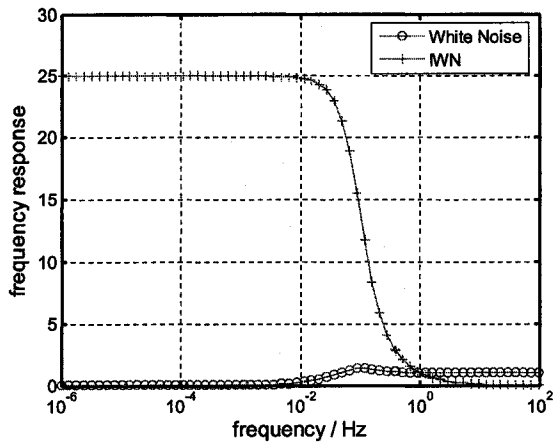

Figure 2.3: *Frequency response of a system with process and controller defined by equations 2.11 and 2.12. Two cases, with and without the presence of IWN are considered*

Figure 2.3 shows the frequency response curves for the two cases. The steady state value the for the case when $N = 1/s$ is clearly non zero, while it tends towards zero for $N = 1$. The next section details the application of this concept in detecting the presence of IWN type disturbance in a system.

2.3 Automatic detecting of IWN type disturbance

The computational aspects of Performance Assessment are carried out in a digital computer using discrete data, hence from here-on we will consider the discrete time version of the above equations. However mixed notations are used in some of the equations for easier understanding and presentation of the concept.

Consider a closed-loop system (equation 2.3) with IWN type disturbance, i.e. $N = \frac{1}{s}$ or $\frac{1}{1-q^{-1}}$ (for the discrete-time case)

$$y_t = \frac{1/\Delta}{1+TQ} a_t \tag{2.13}$$

where, $\Delta = 1 - q^{-1}$. Differencing equation 2.13

$$\Delta y_t = y_t - y_{t-1}$$

$$= \Delta \left(\frac{1/\Delta}{1+TQ} a_t \right)$$

or

$$\Delta y_t = \frac{1}{1+TQ} a_t \tag{2.14}$$

Figure 2.4 shows the frequency response for the two systems represented by equation 2.13 & 2.14.

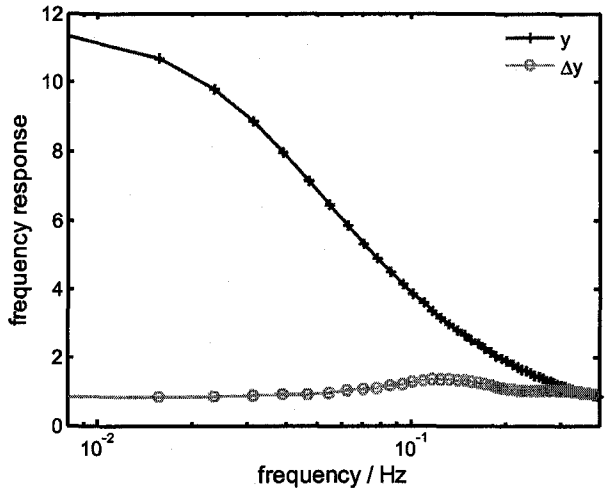

Figure 2.4: *frequency-response of normal (equation 2.13) and differenced (equation 2.14) system with IWN type disturbance,*

Now consider a system with white noise type disturbance

$$y_t = \frac{1}{1+TQ} a_t \tag{2.15}$$

then differencing equation 2.15 gives

$$\Delta y_t = \frac{\Delta}{1+TQ} a_t \tag{2.16}$$

Figure 2.5 shows the frequency response plots for two systems.

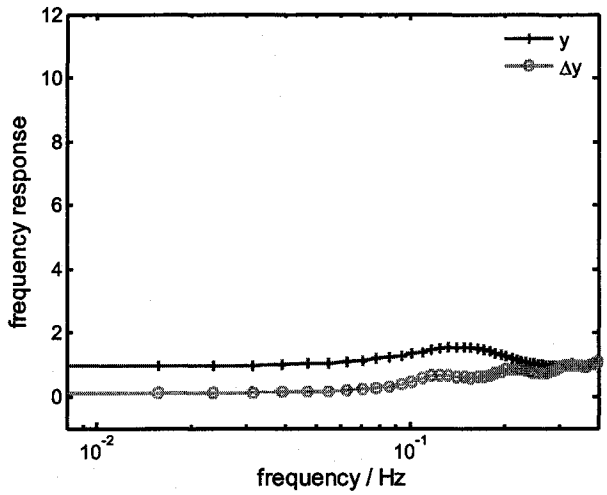

Figure 2.5: *frequency-response of normal (equation 2.15) and differenced (equation 2.16) system with white noise type disturbance*

The difference in the nature of the two plots is clearly visible. For the system with white noise type disturbance, as shown in figure 2.5, the two plots (frequency response of y and Δy) are very similar; the steady state responses tend to zero in both cases. In the case of IWN type disturbance, figure 2.4, the steady state response for y_t tends to a non-zero value while for Δy_t it tends to zero. Hence , by looking at the frequency response plots of the normal and the differenced system (y_t and Δy_t) it is possible to say whether a system has IWN type disturbance or not.

Plotting frequency response curves for a large number of control loops in a typical plant is very tedious, hence automation of the proposed technique is very important. In the next section an index called Low Frequency Amplitude Ratio ($LFAR$), is defined based on which the IWN detection technique can be automated.

2.3.1 Low Frequency Amplitude Ratio

Define,

$$LFAR \triangleq \frac{SS(y_t)}{SS(\Delta y_t)} \tag{2.17}$$

where, $SS(y_t)$ is the steady state response for y_t, and $SS(\Delta y_t)$ is the steady state response for Δy_t

It should be noted that steady state response here means frequency response at a very low frequency. The '0' frequency is practically unavailable from process data. It should be noticed that $LFAR$ for systems with IWN type disturbance is generally high while for systems with white noise type disturbance it is low (see figure 2.4 and 2.5).

Now there are two issues:

- What is the critical value of $LFAR$, above which a system can be said to have IWN type disturbance.
- Is pure integrator ever encountered in real life ?

Addressing the second question first, pure IWN type disturbance is generated if the disturbance model (N) is a pure integrator, i.e.

$$N = \frac{1}{s}$$

or, in discrete domain

$$N = \frac{1}{1 - q^{-1}}$$

but this is rarely encountered in real life. What is more commonly encountered is

$$N = \frac{1 - \alpha}{1 - \alpha q^{-1}} \tag{2.18}$$

where $(1 - \alpha)$ is the normalizing factor. As $\alpha \rightarrow 1$, $N \rightarrow$ pure integrator.

Figure 2.6 shows the variation of $LFAR$ with α for the closed loop system having the transfer function:

$$T = \frac{1}{100s + 1} e^{-\theta s}$$

$$Q = K_c \left(1 + \frac{1}{\tau_I \, s}\right)$$

where $\theta = 30$ and Q is a simple PI controller designed using IMC tunning strategy. Clearly, $LFAR$ increases as α increases.

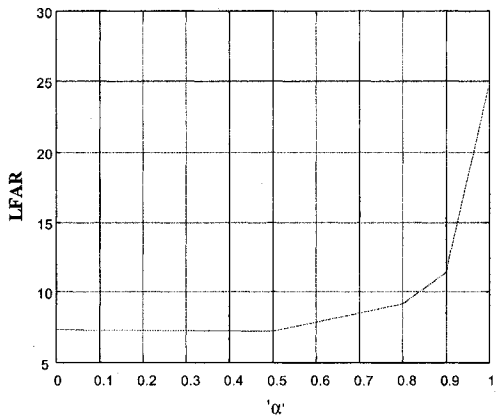

Figure 2.6: *LFAR variation with changing noise model*

Figure 2.7 shows $LFAR$ variation with α for varying $\frac{\theta}{\tau}$ ratio. $\frac{\theta}{\tau}$ ratio is the controllability factor. It can be seen that if α is fixed, $LFAR$ changes for different systems. But in general, for high α values, $LFAR$ is very high. It should be noted that for $\alpha \geq 0.9$ the increase in $LFAR$ is quite steep. Hence, $\alpha = 0.9$ is the critical value above which systems can be treated as having IWN type disturbance. Based on this, a critical threshold value of $LFAR$, $LFAR_{critical}$ is adopted as:

$$LFAR_{critical} = 14 \tag{2.19}$$

Hence for any system if $LFAR \geq LFAR_{critical}$ then the system is considered to have IWN type disturbance, otherwise it does not have IWN type disturbance.

2.4 RPI in presence of IWN type disturbance

As shown in section 2.1 RPI has high fluctuations in presence of IWN type disturbance. This section will now present a modified RPI as calculated in the presence of IWN type disturbance.

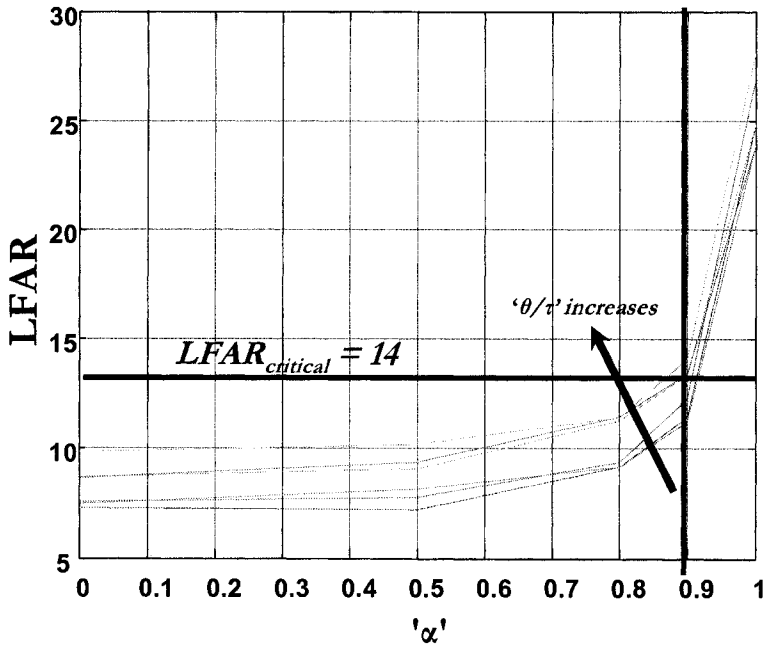

Figure 2.7: $LFAR_{critical}$ *(θ/τ increases as (0:0.1:1))*

RPI based on differenced data and defined as RPI' is found to be stable in presence of IWN type disturbance. Consider a system with IWN type disturbance with no set-point activity. Equation 2.13 describes this system, while equation 2.14 represents the differenced system. RPI' represents the controller performance excluding the effect of the IWN type disturbance.

Figure 2.8 shows RPI of a system with IWN type disturbance, over 10 different data segments. High variation in RPI can be clearly noticed. Figure 2.9 shows RPI for the system calculated using differenced data, i.e. RPI'. RPI' is clearly much stable. The closed loop data is generated using the same SIMULINK block as shown in figure 2.2, with

$$T = \frac{1}{100s+1}e^{-\theta s}$$

$$Q = K_c(1 + \frac{1}{\tau_I})$$

$$N = \frac{1}{1-q^{-1}}$$

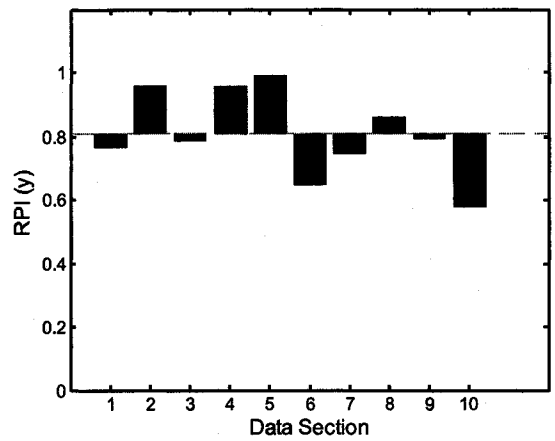

Figure 2.8: *RPI variation for a system with IWN type disturbance*

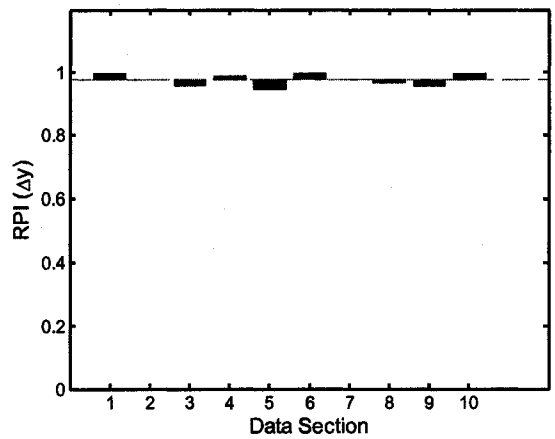

Figure 2.9: *RPI' variation for a system with IWN type disturbance*

In general, when computing RPI, it should be checked if the system has IWN type disturbance, and in that case RPI' should be reported instead of RPI. Figure 2.10 shows a logic flow diagram showing all the steps to be followed before computing RPI or RPI' for a system.

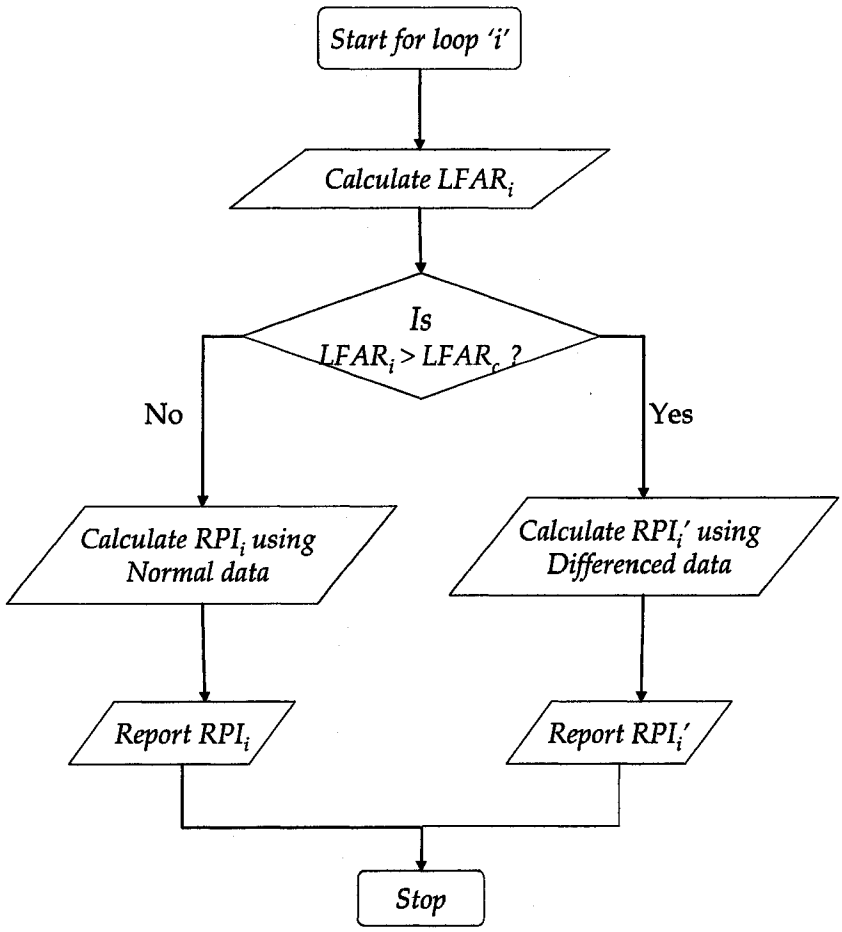

Figure 2.10: *Logic-Flow Diagram for RPI computation*

2.5 Simulation Examples

This section presents a simulation case that demonstrates the application of the concepts developed in the previous sections. Data is generated using the same $SIMULINK$ block diagram shown in figure 2.2, with

$$T = \frac{1}{100s+1}e^{-30s}$$

$$Q_1 = 1.25\left(1+\frac{1}{100s}\right)$$

the simulation is run for 180000 seconds and the data is sampled at a rate of 10 seconds. The system has white noise type disturbance for the first

50000 seconds and IWN type disturbance is introduced thereafter. After 120000 seconds the controller, Q is changed (depicting a change in controller tunning) to

$$Q_2 = 4\left(1 + \frac{1}{50s}\right)$$

Figure 2.11 shows the data generated. The generated data is divided into 17 segments each with 1000 points each. The system is supposed to reach steady state after the first 1000 samples, hence the first 1000 samples are not considered for further analysis. Table 2.1 lists the $LFAR$, RPI (calculated using normal data) and RPI' (calculated using differenced data) values for each of the 17 data segments. The desired settling time is specified as 50 seconds, i.e. 5 samples.

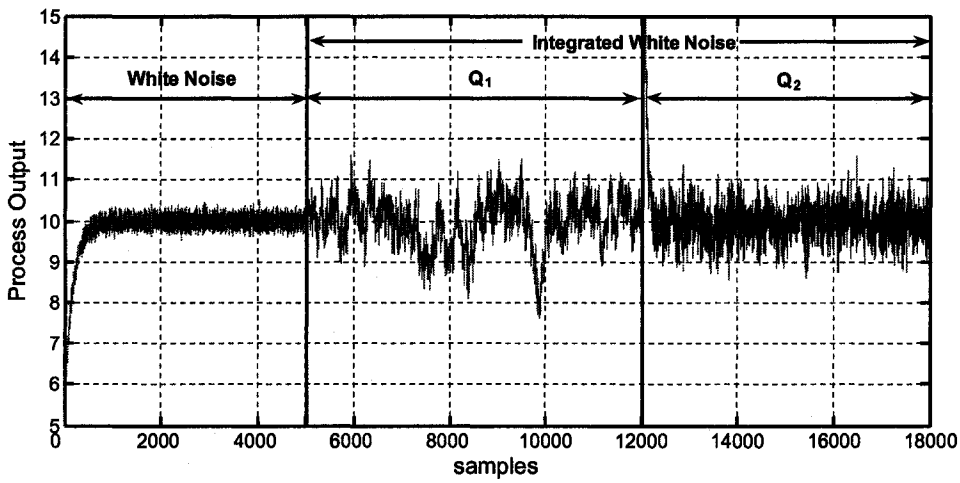

Figure 2.11: *Simulated Data*

Figure 2.12 shows $LFAR$, RPI calculated using the normal data and $RPI_{reported}$ calculated as per the logic shown in figure 2.10 for all the data segments. RPI computed using the normal data shows significant variation after the 4th segment. The change in controller tunning is also not easily detected. It can be seen that $RPI_{reported}$,calculated as per the logic shown in the figure 2.10 is more stable and more importantly the change in controller tunning can be noticed. It should be noted that $LFAR$ fails to detect IWN type disturbance in the last segment (17th) of the data, $LFAR$

Table 2.1: *LFAR, RPI and RPI' estimates for the simulated data segments*

Data Segment	LFAR	RPI	RPI'
1	7.34	0.97	0.98
2	8.2	0.98	0.98
3	7.38	0.97	0.98
4	5.19	0.92	0.97
5	33.35	0.34	0.95
6	22.96	0.4	0.97
7	71.68	0.18	0.94
8	42.75	0.27	0.95
9	104.19	0.15	0.96
10	26.06	0.4	0.95
11	47.72	0.26	0.96
12	34.23	0.41	0.59
13	17.78	0.43	0.45
14	20.83	0.75	0.57
15	20.57	0.76	0.58
16	33.64	0.47	0.52
17	9.55	0.65	0.48

value is less than **14**, see table 2.1. Hence the RPI reported for the last segment is the RPI calculated using normal closed loop data, not RPI' (calculated using the differenced data).

In figure 2.12 RPI for segments 5 - 11 is low in general suggesting low performance. But it is known here that for the first 11 segments the process model does not change and the controller tunning is the same. The only thing that changes is the nature of the noise. As pointed out in Hugo (2006), the changing performance metric (RPI) is solely the result of the changing disturbance, which is not the correct representation of the controller performance. The controller is doing the best it can. RPI' which represents the performance excluding the effect of IWN type disturbance, correctly represents the controller performance during this time.

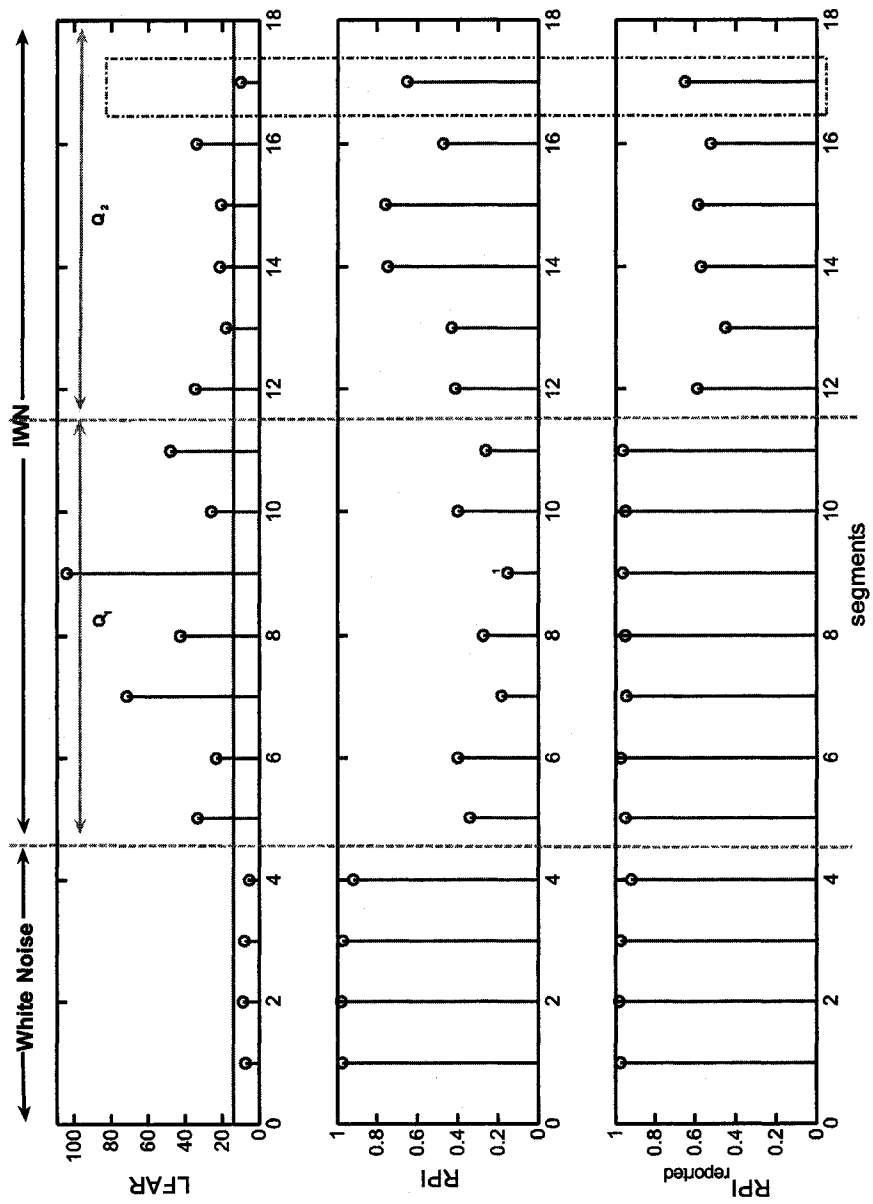

Figure 2.12: *RPI calculated using the normal data over all the data sections*

2.6 Summary

The present work presents a new measure to tackle IWN type disturbances in a control loop in the context of control loop performance monitoring and assessment. The immediate impact of such disturbances on relative performance index (RPI) is shown through simulation case studies. A method has been proposed to automatically detect presence of IWN in a system using $LFAR$, Low Frequency Amplitude Ratio, which is based on the frequency response of the system.

A modification is suggested in the way RPI is calculated for systems with IWN type disturbance. The proposed scheme has been verified on simulation data.

3

Relative Performance Index in presence of High set-point Activity

The previous chapter talked about RPI calculations in a regulatory control environment. The set-point activity was assumed to be negligible. In the present chapter the focus is on controller performance monitoring during high set-point activity. Eriksson and Isaksson (1994) and Swanda and Seborg (1999) have shown that it is desirable to have a separate assessment of performance during set-point changes. Thornhill *et al.* (2003) demonstrated through experimental and industrial examples why the performance during set-point changes differs from the regulatory performance during operation at a constant set-point.

The main contribution of this chapter is to give an insight into the difference between performance assessment during set-point tracking and regulatory cases. It also presents a method to compute RPI during high set-point activity that gives a proper measure of the controller performance in a setpoint tracking mode. The method presented is tested successfully on an industrial case study where it is shown that the conventional way to calculate RPI gives incorrect results while the proposed method gives a correct measure of performance.

3.1 Introduction

Consider equation 3.1

$$y_t = \frac{TQ}{1+TQ} y_{sp} + \frac{N}{1+TQ} a_t \tag{3.1}$$

if there is no set point activity ($y_{sp} = 0$) , then the first term in equation 3.1 can be omitted, i.e.

$$y_t = \frac{N}{1+TQ} a_t$$

the RPI calculations are then based on the simple Autoregressive (AR) model fit to the process output (y_t).

$$(AR) y_t = a_t$$

RPI can be calculated using the impulse response coefficients of the fitted AR model. In cases where the set-point activity is not negligible the first term in equation 3.1 cannot be neglected.

$$err_t = y_{sp} - y_t = \frac{1}{1+TQ} y_{sp} - \frac{N}{1+TQ} a_t \tag{3.2}$$

which can be written as

$$err_t = \frac{1}{1+TQ} (y_{sp} - N a_t) \tag{3.3}$$

Therefore fitting an AR model to equation 3.3 and computing RPI based on this equation would not differentiate between the regulatory or tracking performance. To accurately determine the main mode of controller performance and thus obtain a measure of its performance it is proposed to fit a BJ model to equation 3.1, i.e.

$$y_t = \frac{B}{F} y_{sp} + \frac{C}{D} a_t \tag{3.4}$$

or

$$y_t = P_1 y_{sp} + P_2 a_t \tag{3.5}$$

In the presence of high setpoint activity the main function of a controller is to track the setpoint. Hence RPI calculations should be based on the transfer function P_1. This is defined as RPI_{servo}.

3.1.1 RPI_{servo} Computation

Conventionally, RPI is based on impulse response of the regulatory transfer function. In case of step-point tracking the tracking performance is compared to the desired settling time.

Ideally, the output should exactly match the input, but it is not practically possible due to constraints like, deadtime. For a given desired settling time, $T_{settling}$,

$$P_{desired} = \frac{1}{\tau_s s + 1} \tag{3.6}$$

is the desired closed loop transfer function, where $\tau_s = T_{settling}/4$. Figure 3.1(a) shows the step input and desired (benchmark) output response. For RPI_{servo} calculation, this desired output should be compared to the actual step-response out put of the system.

The benchmark here is the minimum deviation from the input, i.e.

$$benchmark = \sum_{i=0}^{N} (h_i - s_i)^2$$

where, h_i is the step response coefficient of the desired closed loop system, equation 3.6, and s_i is the step-input $[0, 1, 1, 1, 1, ...]$. Figure 3.1(b) shows the benchmark deviation.

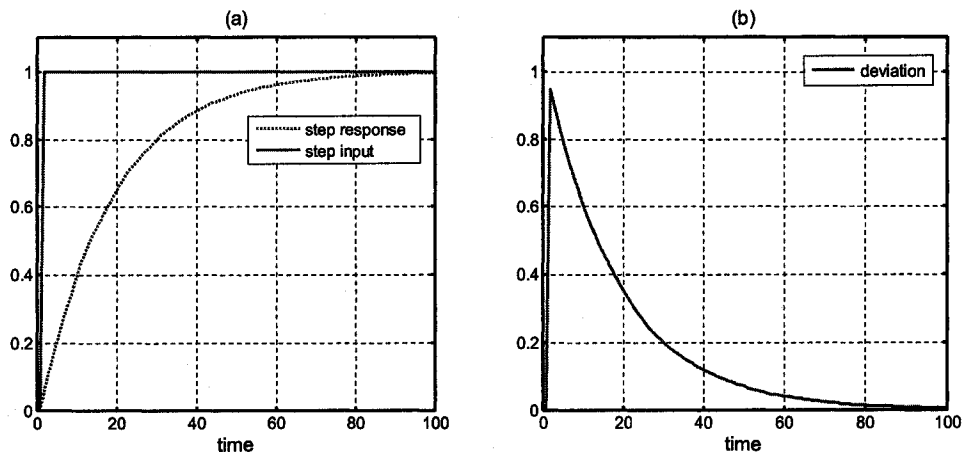

Figure 3.1: *(a) Benchmark Step-response (b) Benchmark deviation*

Therefore RPI for servo problems, RPI_{servo} can be defined as

$$RPI_{servo} \triangleq \frac{\sum_{i=0}^{N}(h_i - s_i)^2}{\sum_{j=0}^{N}(g_j - s_j)^2} \tag{3.7}$$

where, h_i and g_i are the step response coefficients of the desired and the actual transfer functions between y_t and y_{sp}, respectively and $s_i = [0, 1, 1, 1, ., ., ., .]$.

3.2 Industrial case study

Figure 3.2(a) shows flow loop data of an industrial controller. The data is sampled at 15 seconds. Figure 3.2(b) shows the first-half of the data, with high oscillations. The flow control valve was known to have an actuator problem during this time. Figure 3.2(c) shows the data after the actuator problem had been fixed.

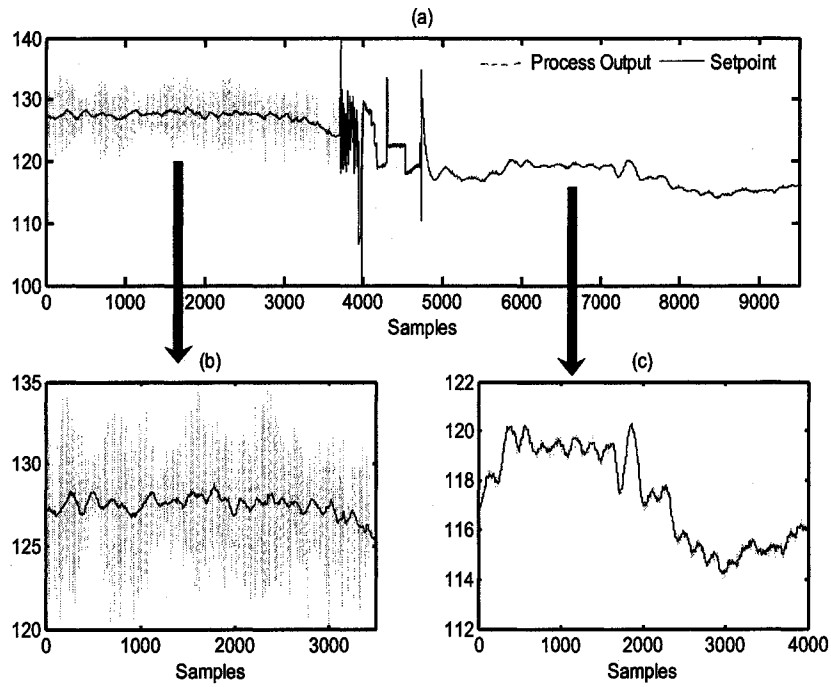

Figure 3.2: *(a) Industrial Flow Loop Data (b) First half of the data, before the problem was fixed (c) Second half of the data, after the problem was fixed*

A BJ model of the order of [3,3,3,3,1] is fitted to the first and the second half of the data, see equations 3.8 and 3.9.

$$y_{t,before} = \frac{6.32z^{-1} - 12.71z^{-2} + 6.45z^{-3}}{1 - 1.61z^{-1} + 0.89z^{-2} - 0.23z^{-3}} y_{sp} + \frac{1 - 0.83z^{-1} - 0.65z^{-2} + 0.73z^{-3}}{1 - 1.72z^{-1} + 0.87z^{-2} - 0.014z^{-3}} a_t \quad (3.8)$$

$$y_{t,after} = \frac{0.34z^{-1} + 0.38z^{-2} - 0.37z^{-3}}{1 - 0.60z^{-1} - 0.08z^{-2} + 0.02z^{-3}} y_{sp} + \frac{1 - 0.61z^{-1} - 0.53z^{-2} + 0.55z^{-3}}{1 - 1.44z^{-1} + 0.68z^{-2} - 0.01z^{-3}} a_t \quad (3.9)$$

Figure 3.3 shows the model prediction (infinite horizon) and the actual output for the first and the second half of the flow loop data. The model predictions for the second half show a 75% fit which confirms a good model quality. For the second half the model quality is not good (5% fit). The main reason for this is the presence of non-linearity in the system (actuator problem).

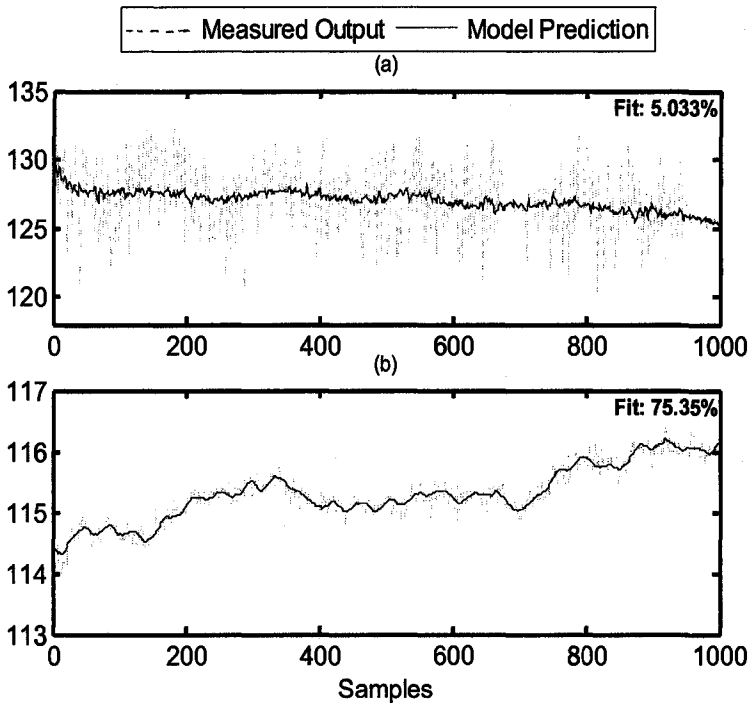

Figure 3.3: *Predicted and the Actual output for (a) First half and (b) Second half of the flow-loop data*

The step response of P_1 and the deviations, for the two cases is very distinct, as shown in figure 3.4. More importantly, the impulse responses of P_2 is almost the same, suggesting that the regulatory performance remains unchanged,see figure 3.5.

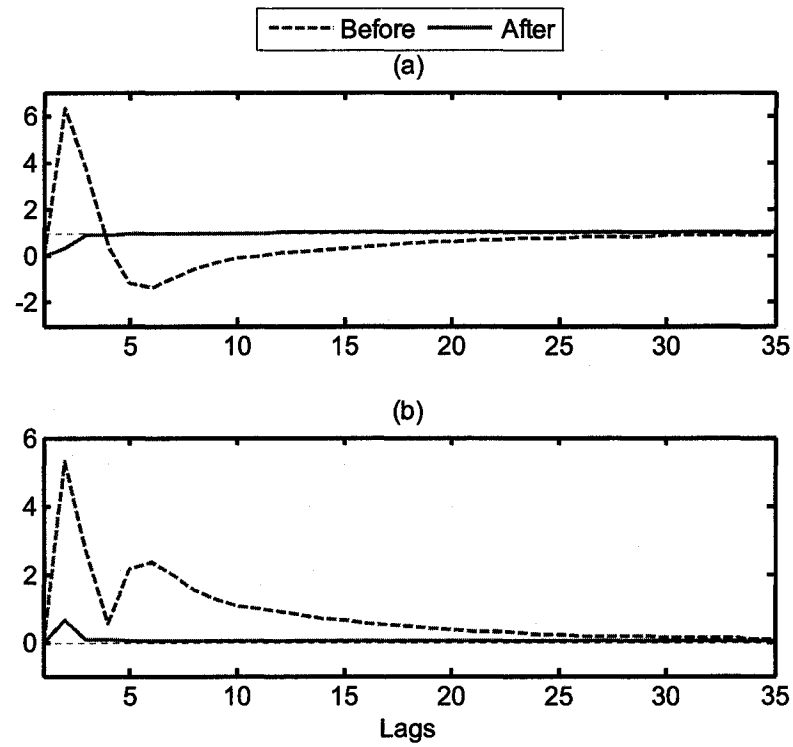

Figure 3.4: *(a) Step-response of P_1 for the 'Before and After' cases (b) Deviation from step-input for 'Before and After' cases*

Table 5.1 lists RPI and RPI_{servo} for first and the second half of the flow loop data. The desired settling time is 60 seconds. RPI fails to distinguish between the performance under the two different scenarios while, RPI_{servo} clearly shows the difference. The low RPI_{servo} value for the second half of the data is mainly due to the low value of the desired settling time of 60 seconds (which was originally used in the plant). For the desired settling time of 120 seconds, the RPI_{servo} for the first and the second half of the data is 0.0053 and 1.36 respectively.

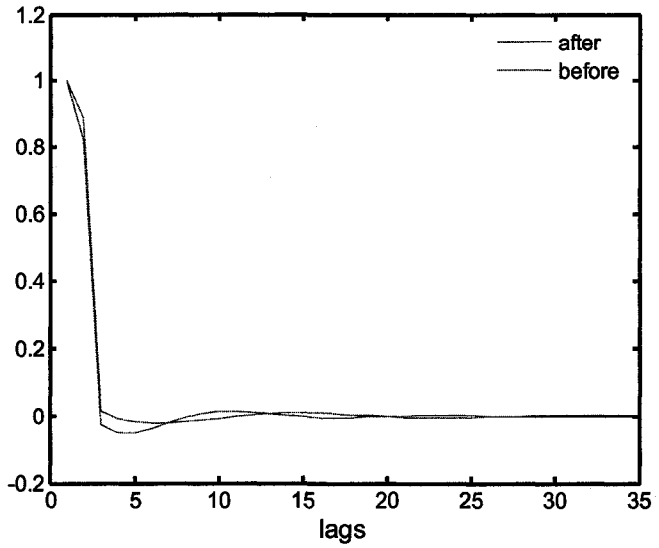

Figure 3.5: *Impulse-response of P_2 for Before and After Case*

Table 3.1: *RPI and RPI_{servo} for Before and After case*

	BEFORE	AFTER
RPI	0.70	0.73
RPI_{servo}	0.0035	0.36

3.3 Summary

This chapter defines a new Relative Performance Index (RPI_{servo}) for cases when set-point activity is high. The new Index is successfully tested on an industrial data set, where it is shown that for cases with high set-point activity the normal RPI does not show the correct controller performance, whereas RPI_{servo} gives a better measure of control performance.

One possible drawback of the proposed method is the estimation of a BJ model, which can be time consuming and certainly hard to automate.

4

Economic Impact of Performance Monitoring

The basic purpose of a controller is to regulate the process such that the process variable tracks the set-point or regulates the loop well in the presence of disturbances. The main objective in tracking or regulatory control is that the process variable should avoid large fluctuations or variability in the control error. Controller performance metrics, such as PI, RPI, RPI' and RPI_{servo}, indicate the performance level of the controller in regulating or setpoint tracking. However, they do not provide information on the economic impact of the control loop and the effect the process variable has on the overall system. Thus, although an important tool, these performance indices by themselves do not give complete information.

For example, a controller with a very low PI may not be very important economically, while a second controller with relatively better PI may be economically very critical, thus a small change in its performance may result in huge financial gains. Therefore, although the first controller demands more attention based on poorer performance, it should be considered as economically less critical than the second controller. Hence a performance metric that combines the performance index with an economic indicator would be helpful in prioritizing the controller monitoring task.

The main contribution of the present work is to give a general method-

ology for computing an index which incorporates controller performance and the economic impact the process variable has on the overall system. This index is defined as Economic Performance Index (EPI).

4.1 Introduction

Previous studies on Economic Performance Assessment deal mainly with cost-benefit analysis of implementing advanced process control systems. In the work by Bauer and Craig (2006), a methodology is proposed for economic assessment of the Advanced Process Control projects. It is stated that most of the direct financial gains from APC are the steady-state gains, i.e. from steady-state optimization. The dynamic control gains are indirect, in the sense that good dynamic control reduces the variability around the operating point, hence allowing closer operation to the optimal point. It is assumed that the variance in the system can be reduced by a fixed amount of 35-50 % through improved control. The work by Muske (2003) introduces the idea of potential reduction in process variance. This potential reduction is based on benchmark control strategies, such as Minimum Variance Control and Internal Model Control. The emphasis here is on cost-benefit analysis of implementing advanced control system.

In the present work, an attempt is made to extend the idea of economic performance assessment as a tool to monitor the day to day performance of the controller. The rest of the chapter is organized as follows. Section 2 summarizes the basic concept of economic gains through variance reduction and introduces the idea of an economic performance index. An industrial example is given in section 3 and section 4 summarizes the findings.

4.2 Economic gains through Variance Reduction

High variance in process variables is never desired. Apart from poor control, this also limits the operating point well below/above the constraint. Hence if the variability in the process variable is reduced the operating point can be moved closer to the constraint, which is generally more economical. Figure 4.1 illustrates this idea.

The first 5000 points in figure 4.1 represent the actual process output of an industrial level loop. Clearly a high standard deviation ($\sigma_{actual} = 4.1$) is

observed; hence the operating point is well above the process constraint. Once the variability is reduced, the operating point can be shifted closer to the economically optimal operating constraint without violating the quality constraint. The second half of the data samples 5000 onwards shows a simulated time-series assuming 50% reduction in the standard deviation ($\sigma^2_{optimal} = 2.05$). This change in the operating point can be easily translated into economic benefit. This is evident also from the distribution curves of the process variable before and after the variance is reduced.

Assuming that the present operating point (set point), $\mu_{present}$ is such that the process is within ±3-sigma limit of the constraints, i.e. the process meets quality constraints 99.5% of the time, the maximum possible change in the operating point (set point) for the illustrative example is given by:

$$opportunity = \mu_{present} - \mu_{optimal} = 3 \times (\sigma_{present} - \sigma_{optimal}) \tag{4.1}$$

The controller performance index (PI) is given by

$$\eta = \frac{\sigma^2_{optimal}}{\sigma^2_{present}} \tag{4.2}$$

Therefore the change in operating point is

$$opportunity = 3\sigma_{present} \times (1 - \sqrt{\eta}) \tag{4.3}$$

The Economic Performance Indicator (EPI) can then be defined as

$$EPI = D \times (opportunity)$$

or,

$$EPI = 3D\sigma_{present} \times (1 - \sqrt{\eta}) \tag{4.4}$$

where, D is the $ gain per unit time period for a unit change in operating point. The gain may be due to several reasons such as, increased productivity or, increased throughput, etc.

It should be noted that it may not be possible to change the operating points in all the cases, e.g. the set-point of an inner loop in a cascade system. The set-point or the operating point to this loop is given by the output of the master controller; hence it cannot be changed. The reduction

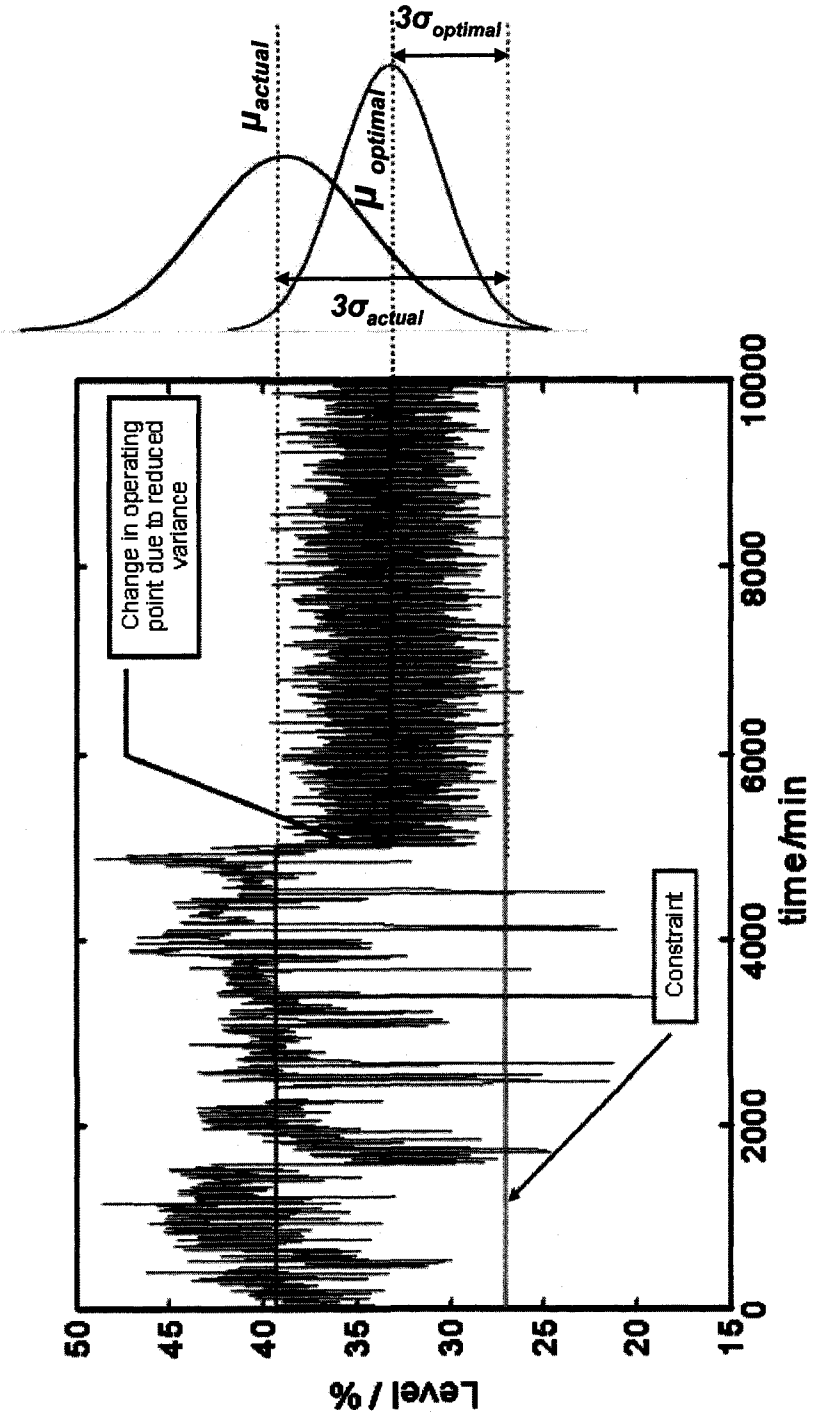

Figure 4.1: *Reduced variance allows us to move the set-point (operating-point) closer to the process constraint, making the process operation more economical*

in variability of the process variable in this case cannot be directly related to economic benefits, unless it occurs through the outer loop.

A level controller in a sump or storage has a different role to play. The objective there is not to reduce variance in the actual level, but rather have the level serve as a buffer to absorb upstream disturbances and in doing so experience higher variability in the level to ensure steady flow out of the sump/storage. In such cases also, the change in operating point is not relevant and thus it cannot be directly translated into economic benefits. However variability from other loops may be transferred to such buffer loops. In this respect an increase in variability in such loops may be an indication of reduced variability elsewhere resulting in economic benefits.

Therefore, classification of the control loops falls into the two main categories, namely

- Movable Operating Point (MOP)
- Immovable Operating Point (IOP)

The next section presents a methodology for online implementation of this technique.

4.3 Implementation Methodology

Equation 4.3 gives the opportunity with respect to the minimum variance control strategy, i.e. the potential change in the operating point if minimum variance control strategy is applied to the system. Operating at minimum variance induces fairly erratic controller action and that may not be desirable. Therefore typically operating under minimum variance control is not desirable. For this reason a de-tuning or correction factor λ is introduced. Therefore the real opportunity (real change in operating point) is λ times the actual opportunity.

$$opportunity_{real} = \lambda \times (opportunity) \tag{4.5}$$

Hence EPI is given by

$$EPI = 3\lambda D\sigma_{present} \times (1 - \sqrt{\eta}) \tag{4.6}$$

Table 4.1 shows a summary of the various stages involved in calculating the EPI. The figures shown in the table are hypothetical. The EPI is calculated using the PI and the user defined correction factor (λ). D, the $ gain per unit opportunity is process dependent.

Table 4.1: *EPI Computation*

Controller Tag	PI	$\sigma_{present}$	Opportunity	λ	Real opportunity	D	EPI
A	0.1	4.9	10	0.5	5	$ 1000	$ 5000

The next section presents the application of the above concepts to an industrial example. The example considered here is located at the primary oil-sands extraction plant at the SUNCOR oil-sands extraction facility in Fort McMurray, Alberta Canada.

4.4 Industrial Case Study

4.4.1 Oil-Sands Extraction Process: An Overview

Extraction is the process whereby oil or bitumen is removed from the oil sand. The oil sand extraction process can be divided into 3 main stages, namely: Slurry Preparation, Primary Extraction and Secondary Extraction.

Slurry Preparation

Slurry preparation is the first step in the oil sand extraction process. The mined tar sands from the mines are fed into tumblers where the bigger chunks are crushed. It then goes into conditioning drums where oil sand is mixed with hot water and caustic soda. Heat is used in the hot water treatment to reduce the viscosity or thickness of the bitumen. Caustic soda helps the attachment of bitumen to the air in the froth formation while releasing it from the sand particles. It essentially helps "clean" the bitumen off the sand. The bitumen then forms small globules that are important in the formation of froth. The slurry passes through a series of vibrating screens that separate and reject any rocks or clumps of clay still in the slurry. It is then pumped into separation tanks.

Primary Extraction

Primary separation occurs mainly in the separation cells. The primary separation cell allows the oil sand slurry to settle out into various layers. The most important of these layers is the bitumen froth layer which rises to the top. The sand (or tailings) sinks to the bottom. The tailings are further processed to extract some more bitumen and then are pumped into tailings ponds. The middle layer (called middlings) consists of bitumen, clay and water. The middlings remain suspended between the sand and the bitumen froth until it is drawn off and put through the second separation vessel called scavenger floatation cell. The scavenger cells extract the remaining bitumen from the middlings.

Secondary Extraction

Bitumen from primary extraction is mixed with a diluent, that thins the bitumen froth so that its density becomes lower than water in the froth. This mixture is then passed through a set of centrifuges where a further separation between bitumen and sand occurs. Adding diluent decreases the viscosity and aids in the speed of separation. The bitumen froth remains in the middle, while the clay, water and sand are thrown to the sides of the centrifuge. The water, sand and clay mixture are pumped out as tailings into the tailings pond. Meanwhile, the bitumen is run through a diluent recovery unit to remove the diluent and sent on to upgrading. The recovered naphtha is returned to the extraction process.

4.5 Plant Description

In this section a brief introduction about plant 3, line 6, which is the primary extraction plant at the SUNCOR facility in Fort McMurray, is given. Figure 4.2 shows a schematic of the plant. The process can be summarized in the following steps:

- The separation cell receives the feed (oil-sand slurry) from feed distributor.
- The overflow from the separation cell is froth, which is mainly bitumen and air.

- The middlings are fine sand particles with traces of bitumen in it.
- The tailings consist of mainly coarser sand particles.
- The forth from the sep-cell goes to the deaerator, where air is separated from froth, before being pumped to the storage tank and then to secondary extraction.
- The middlings from the sep-cell are pumped to scavenger floatation cells, where further separation takes place and the froth is pumped back as sep-cell feed.
- The tailings from sep-cell are pumped to the tailings pump house where after further separation the tailings are pumped into the tailings pond. The tailings stream from floatation cells also joins the tails stream from sep-cell.

Table 4.2 shows list of the critical control loops in line 6 along with the economic category they fall into. These controllers are also marked in figure 4.2

Table 4.2: *List of critical controller in line 6 along with the economic category*

Controller Tag	Description	Category
A	Froth underwash flow controller	IOP
B	Middlings flow controller	IOP
C	PEW addition to sep-cell	IOP
D	PEW addition to tails to maintain density	IOP
E	Sep-cell interface level	MOP
F	Froth launder level controller	IOP
G	Scavenger cell level controller	MOP
H	Deaerator level controller	MOP

4.6 Economic Analysis of MOP controllers

Table 4.3 summarizes the possible shifts in operating point of each of the MOP controller and the economic benefits associated with them. The $ figures have been scaled for confidential reasons.

The detailed explanation about the calculation of the dollar benefits for each of the MOP controller is given below.

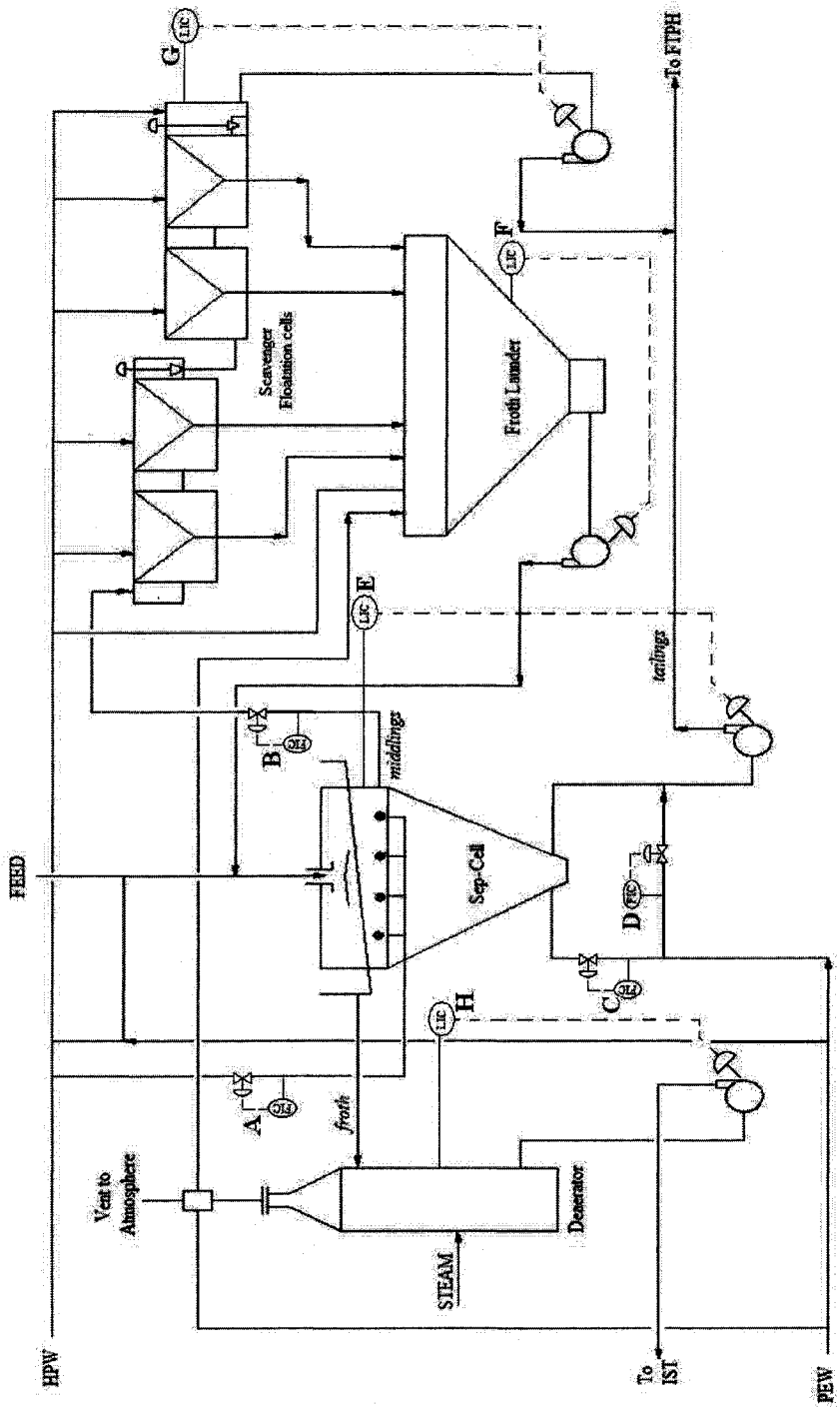

Figure 4.2: *Schematic of Line 6 in plant 3 at Suncor Extraction Plant*

Table 4.3: *Summary of Economic benefits for MOP controllers*

Controller Tag	PI	$\sigma_{present}$	λ	Real opportunity	D	EPI	$ Gains/year
E	0.31	4.8	0.5	3.19	667	$ 2,131	$ 777,839
G	0.93	2.6	0.5	0.14	667	$ 93	$ 34,084
H	0.26	9.5	0.5	7.0	700	$ 8,183	$ 2,986,795

E: Separation Cell interface level

Controller 'E' controls the interface, (interface between the froth and middlings), level in the separation cell. This level plays a critical role in both froth recovery, and quality. High interface level means higher residence time for oil-sand slurry in the sep-cell, hence higher recovery. However very high interface level causes a large amount of sand (fines) to enter into the overflow stream, thus affecting the quality of the product (froth). If the interface level is low, large amount of bitumen is lost in the tails, thus reducing the recovery.

The ideal operating condition is to maintain the interface level as close as possible to the high level mark. The high level mark is the level at which a significant quantity of sand (fines) starts to enter the overflow stream. Figure 4.3 shows the effect of changing the operating point graphically.

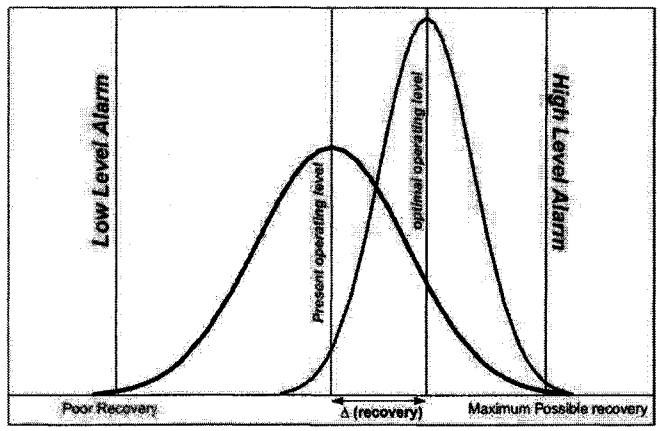

Figure 4.3: *Change in operating level directly relates to the economic gains*

The following empirical relationship between % recovery and % level

has been established by Suncor personnel

$$y = 1.3x + 32 \tag{4.7}$$

where y is the % recovery and x is % level. This expression is used to tabulate Economic benefits in tables 4.4 and 4.5.

Table 4.4: *E: Economic benefits*

Increase in bitumen recovery/ unit increase in level	1.3%
Average bitumen processed per day	1000 barrels
Gain per unit increase in level (D)	$ 667
Performance Index	0.31
$\sigma_{present}$	4.8
Opportunity	6.39
Correction factor (λ)	0.5
Real opportunity	3.19
EPI	$ 2,132
Potential $ gain per year	$ 778,227

G: Scavenger floatation cells level

Middlings from the sep-cells are pumped into the scavenger floatation cells where further separation occurs. The level here plays the same role as that in sep-cell. Table 4.5 summarizes calculation of the economic benefit associated with controller 'G'.

Table 4.5: *G: Economic benefits*

Increase in bitumen recovery/ unit increase in level	1.3%
Average bitumen processed per day	1000 barrels
Gain per unit increase in level (D)	$ 667
Performance Index	0.93
$\sigma_{present}$	2.62
Opportunity	0.28
Correction factor (λ)	0.5
Real opportunity	0.14
EPI	$ 93
Potential $ gain per year	$ 34,101

H: Deaerator Level Controller

Froth from the sep-cell has a lot of air in it and hence cannot be pumped easily, as it causes cavitation. Therefore separation of air from froth is required before it can be pumped to the Inter Stage Tank. Steam is used to separate air from froth. In the deaerator, steam comes in direct contact with the froth; air separates and is vented out to the atmosphere.

Controller 'H' controls the level of froth in the deaerator. The direct benefit of better level control here comes from the fact that lower the level in deaerator, more steam is lost. Figure 4.4 shows the deaerator with the high level and low level marked as 80% and 20% respectively. It is known that at 20% absolute level, all the steam is lost and at 80%, no steam is lost. It is also known that steam loss varies linearly with the level. Hence, steam saving / unit increase in level can be calculated as

$$\text{steam saving / unit increase in level} = 1.67$$

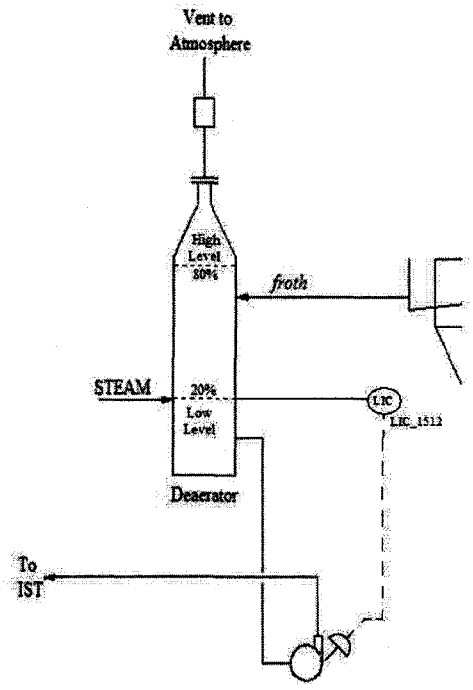

Figure 4.4: *Deaerator schematic showing the upper and lower bounds of the level*

Figure 4.5 graphically demonstrates the effect of shifting the operating level closer to the high level mark. The economic benefit calculations are summarizes in table 4.6.

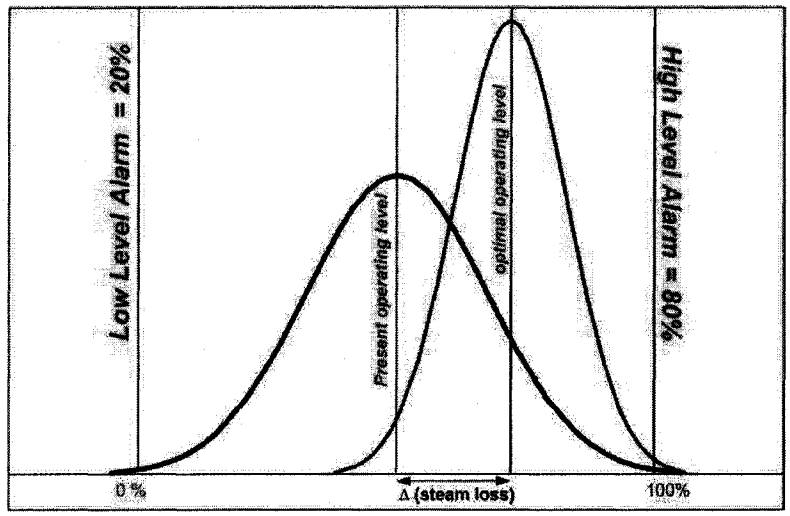

Figure 4.5: *Change in deaerator level directly relates to the change in steam loss*

Table 4.6: *H: Economic benefits*

Steam saving / unit increase in level	1.67%
Average steam flow per day	1000 Mlb
Gain per unit increase in level (D)	\$ 700
Performance Index	0.26
$\sigma_{present}$	9.5
Opportunity	14
Correction factor (λ)	0.5
Real opportunity	7
EPI	\$ 8,183
Potential \$ gain per year	\$ 2,986,795

4.7 Summary

The concept of Economic Performance Indicator developed in this work compliments the current Performance Indices. The EPI gives dual information, the present controller performance and the potential economic

impact of improved control on the overall system. Hence, EPI is the correct representation of the controller health in the context of the system as a whole. This idea is demonstrated using an industrial example. The EPI computed is based on the Performance Index (PI) of the controllers. Controllers 'E' and 'H' have almost the same level of regulatory performance but EPI shows that maintaining controller 'H' is far more critical compared to controller 'E'.

As discussed above, EPI is dependent on the present controller performance and can be easily automated, thus making it easy to implement. The proposed scheme can be summarized in the following steps:

1. Classify the controllers as MOP or IOP.
2. Compute Performance Indices for each of the MOP controllers and identify applicable constraints and room to change operating points.
3. Based on the PI, compute the opportunity for each of the MOP controllers.
4. EPI can then be computed based on process knowledge.

5

Quantification of Valve Stiction

A control valve is one of the few or occasionally the only moving part in a control loop, and therefore it is most prone to mechanical problems. This chapter deals with one such very common control valve problem, stiction. Figure 5.1 shows a cross section of a spring-diaphragm valve (which is most widely used in process industry). The purpose of packing in the valve is to make sure the fluid does not leak into the stem section of the valve, which may cause safety issues. Over-time due to wear and tear, high static friction develops between these packings and the wall of the valve. This high *st*atic-fr*iction* or STICTION hinders the smooth movement of the valve stem.

High static-friction or stiction in control valves is a major cause of oscillations in control loops, which result in poor performance. This may lead to higher rejection or off-spec products which means considerable amount of economic loss. Therefore, the correct diagnosis of stiction is important. There are several methods for detecting stiction, (Taha *et al.* (1996), Wallén (1997), Horch and Isaksson (1998), Choudhury *et al.* (2004*c*), Choudhury *et al.* (2004*b*), Horch (1999), Singhal and Salsbury (2005), Stenman *et al.* (2003), Srinivasan *et al.* (2005*a*), Srinivasan *et al.* (2005*b*)), but quantification of stiction still remains a challenge.

Earlier work by Choudhury *et al.* (2004*b*) quantifies stiction by fitting an ellipse to the process output (pv)- controller output (op) plot and the

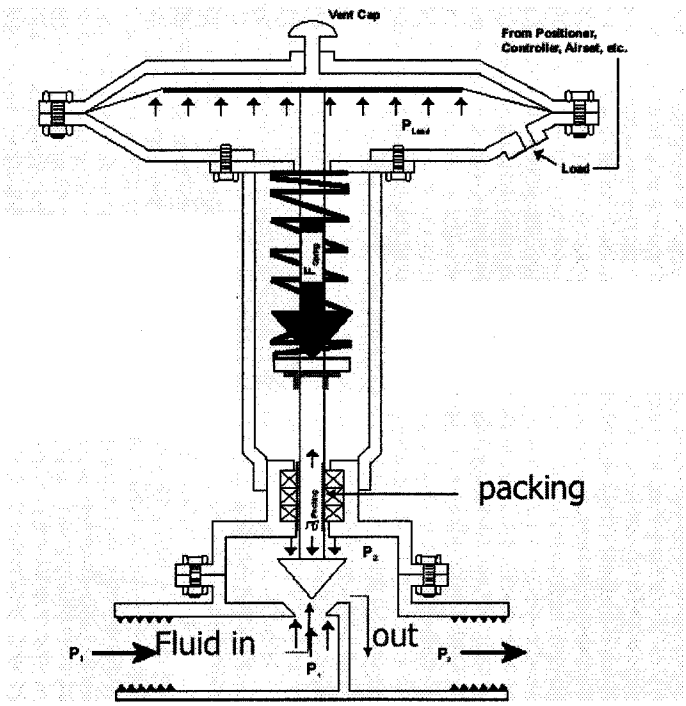

Figure 5.1: *Cross Section of a spring-diaphragm valve*

maximum width of the ellipse is reported as 'apparent stiction'. Recently, Srinivasan *et al.* (2005*a*) introduced another approach where they exploited the fact that the presence of stiction has distinct qualitative shapes or pattern in the controller output, *op* and the controller variable, *pv* signals. They have applied a pattern recognition technique using Dynamic Time Warping (*DTW*) on the *pv* and *op* data. First, the test patterns (for both *op* and *pv*) are generated using the zero crossing data from the raw signals. Then these test patterns are compared to the actual signal. If stiction is confirmed then the maximum peak-to-peak amplitude is reported as stiction. However, the maximum peak-to-peak amplitude is just the magnitude of limit cycle and cannot be attributed to real stiction. Another disadvantage with this approach is the apriori knowledge of the patterns in the *op* and *pv* due to stiction. The patterns described therein may not be always due to stiction. Some of those patterns in the *pv* and *op* signals may arise simply due to the presence of a tightly tuned controller or an oscillatory disturbance. In addition to these, asymmetric stiction, which is not uncommon, cannot be detected and quantified using this approach.

In another method proposed by Srinivasan *et al.* (2005*b*), a Hammerstein model identification approach is explored. A general structure of a Hammerstein model is shown in figure 5.2. The non-linear part of the Hammerstein model is described by a single parameter stiction model (Stenman *et al.* (2003)).

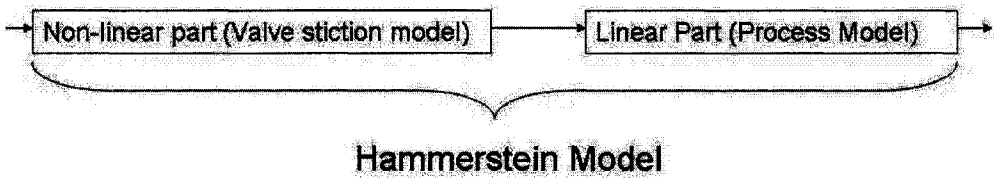

Figure 5.2: *General Structure of a Hammerstein Model*

It has been observed that the single parameter stiction model does not depict the true stiction behavior (Choudhury *et al.* (2004*a*)) as discussed in section 2. In this study, the proposed approach uses a two parameter stiction model proposed by Choudhury *et al.* (2004*a*) to model the non-linear component of the Hammerstein model.

The rest of the chapter is organized as follows: In the next section a brief discussion of the two parameter stiction model is provided. This is followed by an example demonstrating the importance of slip-jump, J, in loop dynamics. Then the proposed method is presented followed by simulation, experimental and industrial results.

5.1 Why use a two parameter Model of Stiction?

This section briefly discusses the adequacy of a two parameter stiction model for closed loop simulation of stiction. Also, the limitations of the one parameter stiction model proposed by Stenman *et al.* (2003) and used in Srinivasan *et al.* (2005*b*) are briefly discussed. Before discussing the data-driven stiction models, a case of an industrial example where a valve was sticky is presented in order to find the right pattern of stiction present in a valve operating under closed loop control configuration.

5.1.1 An industrial control loop with a sticky valve

Consider a level control loop which controls the level of condensate in the outlet of a turbine by manipulating the flow rate of the liquid condensate. The control valve of this loop is confirmed to have stiction. In total 8640 samples for each tag were collected at a sampling rate of 5 s. Figure 5.3 shows a portion of the normalized data. The left panel shows time trends for level (*pv*), the controller output (*op*) which is also the valve demand, and valve position (*mv*) which can be taken to be the same as the condensate flow rate. The plots in the right panel show the characteristics *pv-op* and *mv-op* plots. The bottom figure clearly indicates both the stickband plus deadband and the slip jump effects. The slip jump is large and visible from the bottom figure especially when the valve is moving in a downward direction. It is marked as 'A' in the figure. The *pv-op* plot does not show the jump behavior clearly because the process dynamics (i.e., the transfer function between *mv* and *pv*) destroys the pattern. The pattern shown in the actual valve position (*mv*) vs. controller output (*op*) can be taken as a typical signature of valve stiction because it clearly shows the deadband plus stickband and the slip-jump. Similar patterns can be found in many industrial control valves suffering from stiction.

5.1.2 One-parameter stiction model

A simple one parameter stiction model was proposed by Stenman *et al.* (2003). The model can be mathematically expressed by the following equation

$$x(t) = \begin{cases} x(t-1) & ,if \mid x(t) - d \mid < d \\ u(t) & \text{otherwise} \end{cases}$$

Where, *x(t)* and *x(t-1)* are the valve output (stem position) at time *'t'* and *'t-1'* respectively, *u(t)* is the controller output at time *'t'* and *'d'* is the valve stiction band. For details of this stiction model, interested readers are referred to Stenman *et al.* (2003).

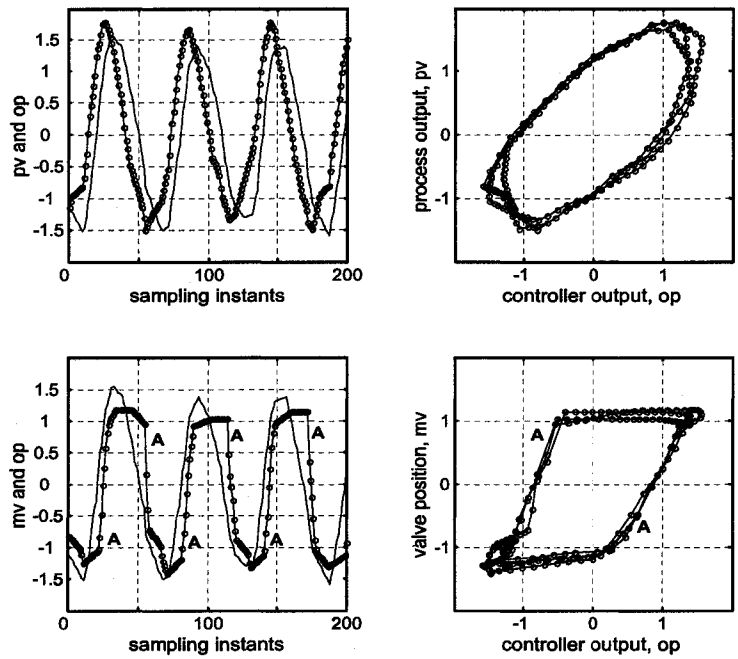

Figure 5.3: *Normalized industrial flow loop data, the line with circles is pv and mv, the thin line is op*

5.1.3 Two-parameter stiction model

A two parameter model proposed by Choudhury *et al.* (2004*a*) captures the stiction phenomenon successfully. The two parameters are: S (Stickband + Deadband) and J (Slip-jump). For details on this stiction model interested readers are referred to Choudhury *et al.* (2004*a*).

5.1.4 Comparison between one-parameter and two parameter stiction model

Figure 5.4(a) shows a typical valve output (mv), vs. controller output (op) plot for the one parameter stiction model described in Stenman *et al.* (2003) and Srinivasan *et al.* (2005*b*) while Figure 5.4(b) shows the same plot for the two parameter stiction model proposed in Choudhury *et al.* (2004*a*). Figure 5.4(a) is clearly different from the pattern of stiction shown in Figure 5.3. It suffices to say that the one parameter stiction model does not

capture the true characteristic of stiction. Indeed it should not be called a stiction model, rather it should be defined as a quantization or a staircase function. On the other hand, the plot for two parameter stiction model (Figure 5.4(b)) clearly matches with the pattern in Figure 5.3. Thus the two parameter stiction model is able to adequately capture the characteristic of valve stiction (Choudhury *et al.* (2004*a*).

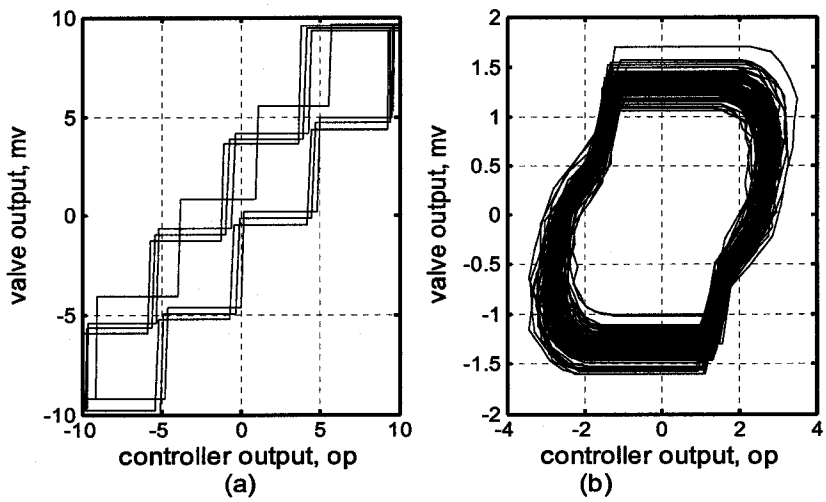

Figure 5.4: *(a) mv-op for one parameter model ('d') (b)mv-op for two parameter model (S, J)*

5.2 Issues in quantifying stiction

5.2.1 Effect of controller dynamics and process dynamics on apparent stiction

Earlier work by Choudhury *et al.* (2004*b*) and Choudhury *et al.* (2005) quantifies stiction by fitting an ellipse to the *pv-op* plot and the maximum width of the ellipse is reported as 'apparent stiction'. Stiction is reported as 'apparent' because the estimate includes the effect of the process and controller dynamics. The following simulation example demonstrates the effect of the controller tuning on the estimation of apparent stiction.

Figure 5.5 shows the simulink block diagram used for generating stic-

tion data. The process model is

$$G(z) = \frac{1.45z - 1}{z^4 - 0.8z^3} \tag{5.1}$$

The controller is implemented in the following form:

$$C(s) = K_c \left(1 + \frac{1}{\tau_i\, s}\right) \tag{5.2}$$

The reset time, τ_I, is fixed at 1 sec and the gain,K_c, is varied.The Stiction parameters 'stickband+deadband', S and 'slip jump', J are fixed at 3 and 1, respectively. Three cases, K_c = 0.05, 0.10 and 0.15, are considered and 1024 samples are generated for each case.

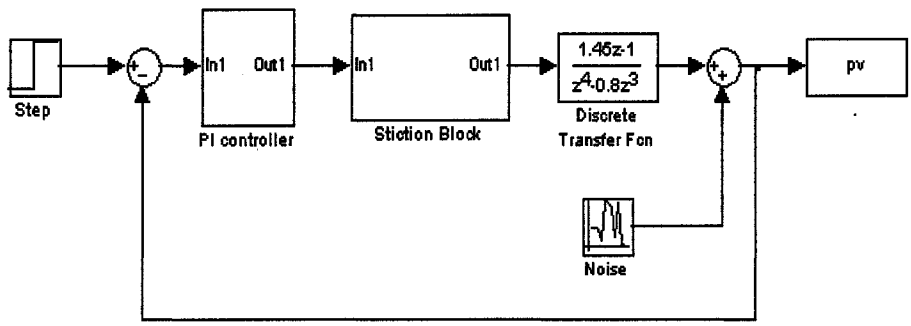

Figure 5.5: *Simulink block diagram used for generating stiction data*

Figure 5.6 shows the *pv-op* plot and the fitted ellipse for the three cases. The apparent stiction reported are: for K_c = 0.05, 0.10 and 0.15, the estimated apparent stiction are 5.79, 3.06 and 1.62, respectively. Ideally, it should be same because the same amount of stiction was used for all cases (S=3 and J=1). A similar effect of the process dynamics can also be observed on the value of apparent stiction. Hence the width of the ellipse in the *pv-op* plot termed as 'apparent stiction' cannot be taken as an accurate estimate of stiction.

5.2.2 The importance of quantifying Slip-Jump (J)

Describing function analysis performed in Choudhury *et al.* (2004*a*) suggests that for processes without any integrator, limit cycles in a control

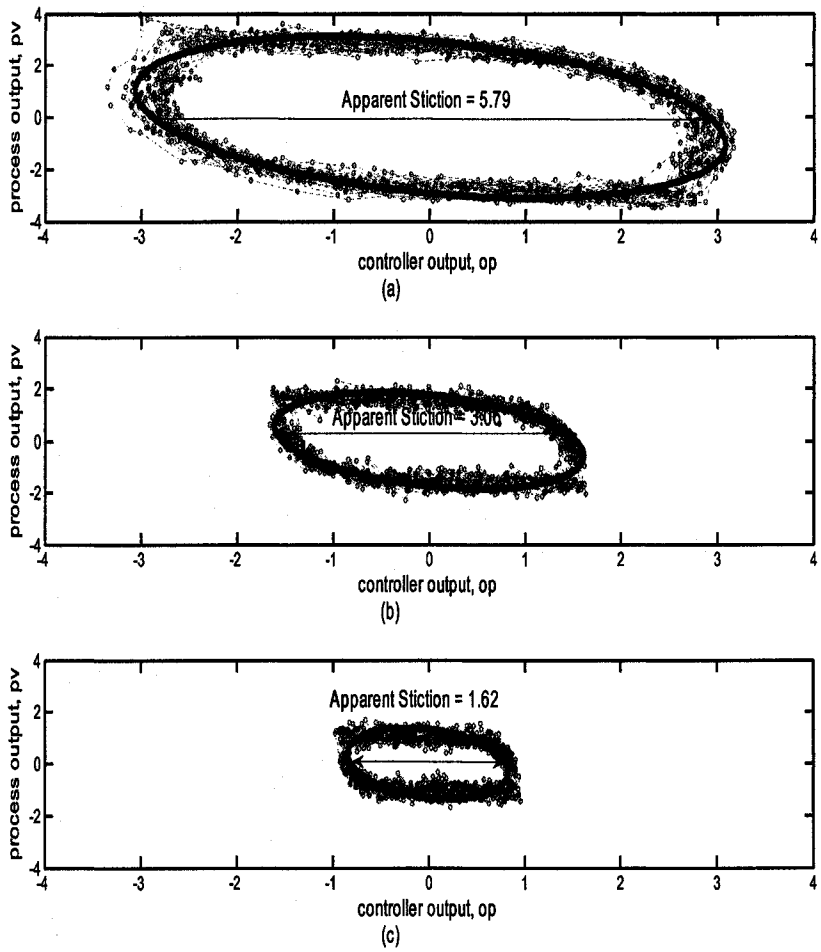

Figure 5.6: *mv – op plot and fitted ellipse (a)* $K_c = 0.05$ *(b)* $K_c = 0.10$ *(c)* $K_c = 0.15$

loop may occur only in the presence of slip-jump (J) for the case of a sticky valve. Moreover, the amplitude and frequency of the limit cycles depend significantly on the slip-jump (J). The following simulation results show the effect of J on the amplitudes and frequencies of the limit cycles.

The system considered here is the same as in Section 5.2.1. In order to observe the impact of J clearly, the controller parameters are chosen as K_c = 0.15 and τ_I = 0.15 sec.

Figure 5.7 shows the variation of the frequency and amplitude of limit cycles with slip jump (J) keeping S constant ($S = 6$). For each case, 1024 points were collected. No oscillations are observed for the case when there is no slip-jump, i.e. J=0. Periods of oscillation (T_p) are 250 s, 111 s and 72 s for values of $J = 1$, 3 and 6, respectively. From this simulation study, it is clear that both amplitude and frequency of limit cycles increase with the increase of J. Therefore, the estimation of J is as important as the estimation of S.

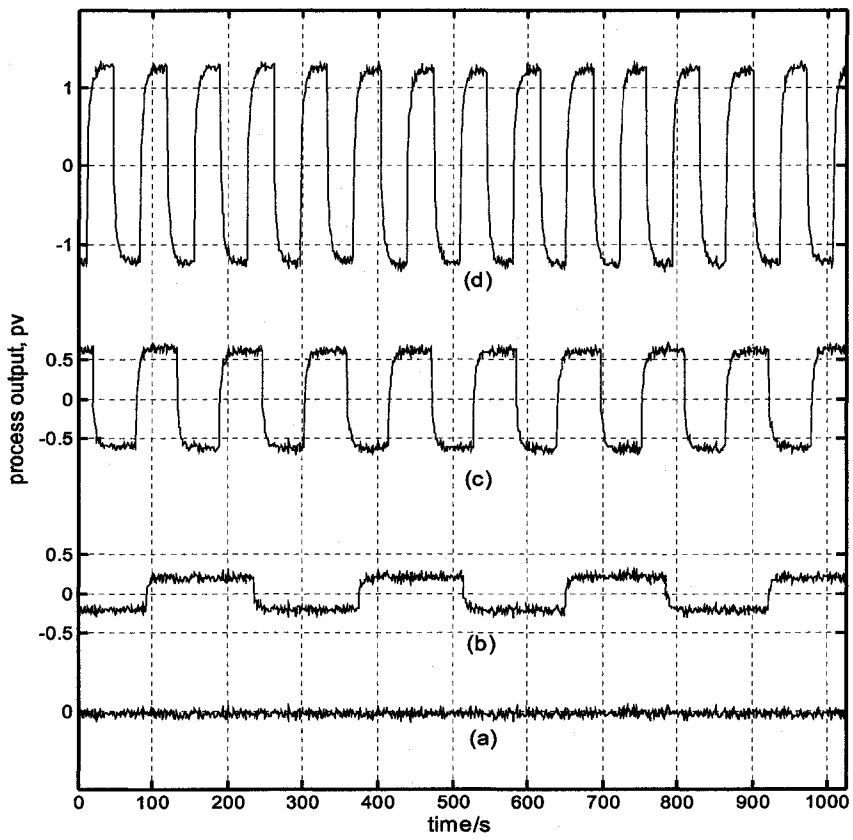

Figure 5.7: *(a) J=0, no oscillations detected (b) J=1, T_p=250, amplitude=0.20 (c) J=3, T_p=111, amplitude=0.60 (d) J=6, T_p=72, amplitude=1.20.*

5.3 Methodology for simultaneous Estimation of S and J

Figure 5.8 shows the detailed flow chart of the procedure for estimating 'S' and 'J'. This is an iterative optimization procedure to identify both the stiction model parameters and the process model simultaneously. The controller output data (op) is supplied to the two parameter stiction model to obtain the actual valve output or valve-postion data, (vo), for a fixed value of S and J. Then, the predicted valve output, vo, and the process output data, (pv), are used to identify the process model using Akaike's Information Criteria (AIC). The procedure is repeated for various values of S and J obtained from a two dimensional grid search. The value of S and J that gives minimum mean square error for the controlled process variable (pv) is reported as stiction. Other global search methods such as Simulated Annealing were also tried but resulted in higher computational time. The details of the algorithm are as follows:

- Import process ouput, pv and the controller output, op.
- Check for non-linearity in the system. In this work the bicoherence based method proposed by Choudhury *et al.* (2002) is used for non-linearity detection.
- Choose a value for (S_i,J_i) from a two dimensional grid of S and J.
- Use the controller output, op, data and the two-parameter stiction model with chosen (S_i, J_i) to compute the valve output, vo. This is the non-linear part of the Hammerstein model.
- Identify the process model (linear part of the Hammerstein model) using the valve output, vo, and the process output, pv.
- Then the process output is predicted (pv') using the identified process model and the computed valve output, vo.
- Compute the Mean Squared Error between the predicted and the actual process output

$$MSE(S_i, J_i) = \sum_{i=1}^{N} (pv_i - pv_i')^2 \tag{5.3}$$

- MSE is computed for all the points in the grid of S and J. The value (S_m, J_m), for which MSE is minimum, is reported as stiction.

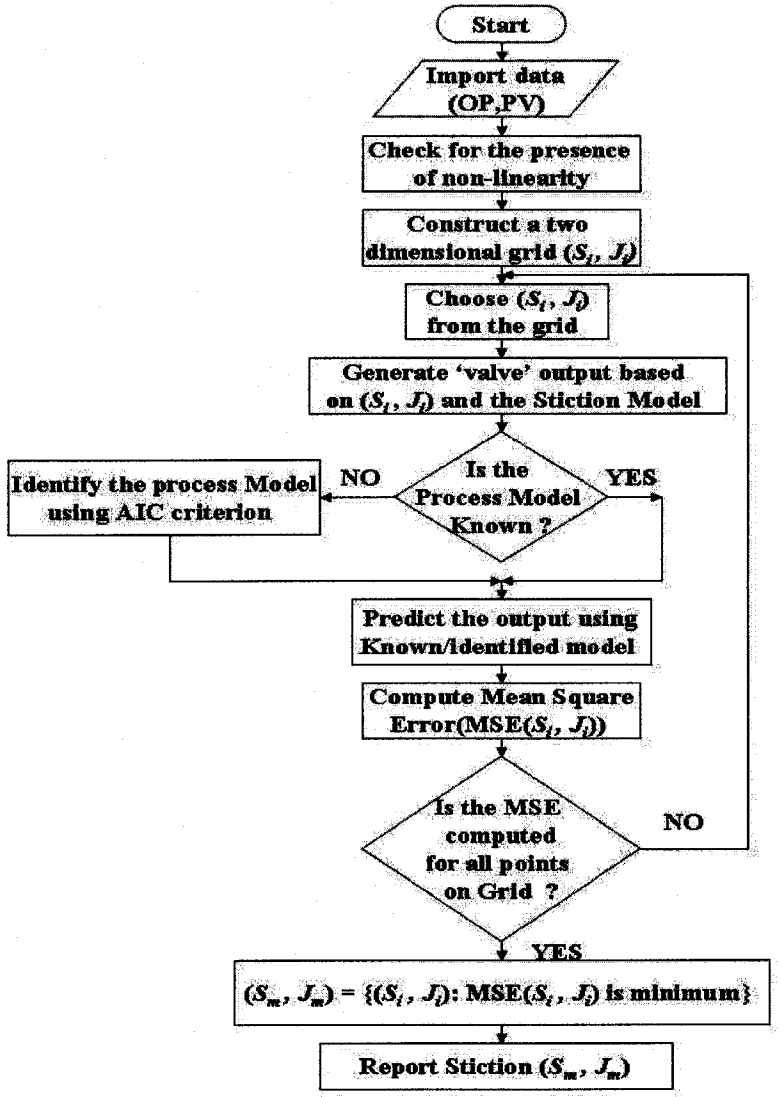

Figure 5.8: *Logic flow diagram of the proposed method*

The following important points should be considered in the implementation of the method:

- The prediction, using the identified or known model and the valve output, is done using a one-step-ahead predictor. The purpose of us-

ing one-step-ahead predictor is that this makes the overall procedure less dependent on the process model, estimation of which is of less interest for this case.

- There is a possibility that for a particular value of (S, J) the computed valve output may be saturated. In this case the identification of the linear part of the Hammerstein model would be difficult because the input signal would not be persistently exciting. This may result in erroneous results. Therefore, before using the valve output (vo) for the identification of the process model, the signal should be examined for possible saturation.

5.4 Results from Simulation Studies

All simulations were performed using the same system described in Section 5.2.1. The controller gain, $K_c = 0.15$ and $\tau_I = 1$ are fixed. Two scenarios are considered here. First, when the process model is known i.e. the linear component of the Hammerstein model is known. Second, when the linear part of the Hammerstein model is unknown and estimated along with the nonlinear part.

Table 5.1 shows the estimation results using the proposed method. It is assumed that the process model is known. The estimated values are close to the actual values.

Table 5.1: *Comparison of actual and estimated S and J (known model case)*

S		J	
Actual	Estimated	Actual	Estimated
1	1	0	0
1	1	1	1
4	4	2	2
6	6	4	3.5
8	8	8	8
8	8	10	10
10	8	2	0

Table 5.2 shows the estimation results when an external disturbance is added to the system with sticky valve. A sinusoidal input with a frequency of 1 rad/sec and amplitude of 1 is used as external disturbance.

The process model is assumed to be known. The estimation is exact in most cases. This indicates that the proposed method is able to quantify stiction even in presence of external oscillations.

Table 5.2: *Comparison of actual and estimated S and J in the presence of external oscillations (known model)*

S		J	
Actual	Estimated	Actual	Estimated
1	1	1	1
4	4	2	2
6	6	4	4.5
10	10	5	5
12	12	4	4
12	13	0	1

In Table 5.3 estimation results are shown when the data is corrupted by noise (random noise with zero mean). Signal to noise ratio (SNR) is computed as the ratio of the variance of the noise free signal to variance of the noise. For this the value of S and J are fixed to 6 and 4 respectively and the data is simulated with different noise levels in the system. The results show that the method is relatively insensitive to the presence of noise, and therefore it should work well when applied to real process data.

Table 5.3: *Prediction in presence of noise (S = 6 and J = 4) (known model)*

SNR	Estimated (S)	Estimated (J)
100	6	3.5
50	6	4
25	6	4
12.5	6	4
10	6	3.5

Table 5.4 shows the results for the case when it is assumed that the process model is not known. The algorithm was not supplied with the process model. For all cases, S has been estimated correctly except when $S < J$ $(S = 4, J = 8)$. But such cases, where $J > S$, are rarely encountered in real life. Slip-jump is also estimated correctly for most cases.

Table 5.4: *Comparison of actual and estimated S and J, unknown model case*

S		J	
Actual	Estimated	Actual	Estimated
1	1	0	0.5
4	4	2	2
6	6	4	4
10	10	10	7.5
10	10	8	8
10	10	2	2
4	2	8	8

5.5 Results from Pilot Plant Experiments

For the verification of the proposed method, data was generated using a laboratory scale setup of a tank system in the Computer Process Control Laboratory in the Department of Chemical and Materials Engineering at the University of Alberta. Data is generated for two control loops: flow and level(cascade) control.

5.5.1 Flow Control Loop:

The schematic of the process is shown in Figure 5.9. First of all, the control valve was checked for possible presence of stiction using the so called bump test or the valve travel test and it was found to be stiction free. Then the two-parameter stiction model was used to introduce valve stiction within the software as shown in Figure 5.9.

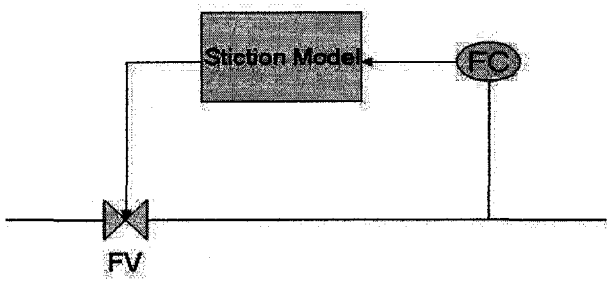

Figure 5.9: *Schematic for the Flow loop*

The signal from the flow controller (FC) is supplied to the stiction model (with already known S and J). The output of the stiction model is then provided to the flow control valve (FV).Figure 5.10 show the process output (pv) and the controller output (op) for the system for $(S, J) = (2, 1)$. Clearly, stiction introduces limit cycle behaviour in the loop. The results of stiction estimation are provided in Table 5.5. Two cases are considered for this loop. For both cases, estimated S and J are in relatively good agreement with the actual S and J.

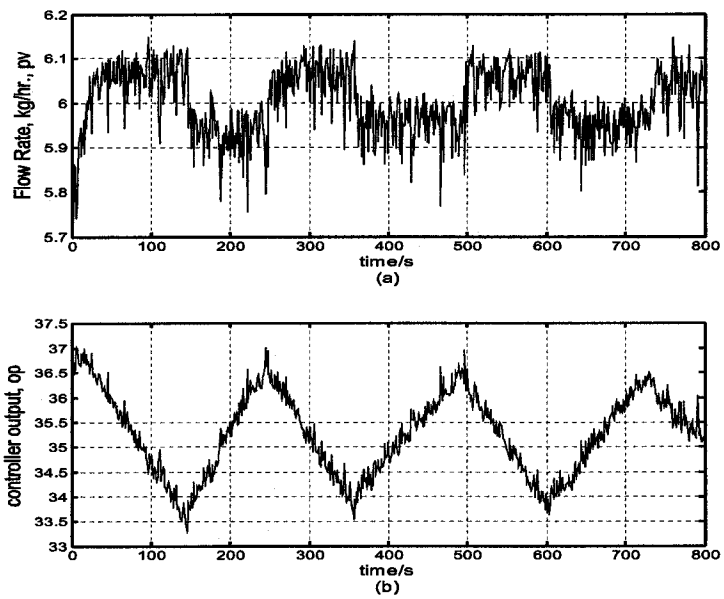

Figure 5.10: *Process output (flow rate, PV) and controller output (OP) for the flow control loop*

5.5.2 Level Control Loop:

The schematic of the control loop is shown in figure 5.11. This is a cascaded loop. The level controller (LC) signal acts like a set point for the flow controller (FC). Process output (pv, the level) and the controller output (op) for $(S, J) = (1, 1)$ are shown in Figure 5.12.Results of stiction estimation are summarized in Table 5.5. The method successfully quantifies S and J.

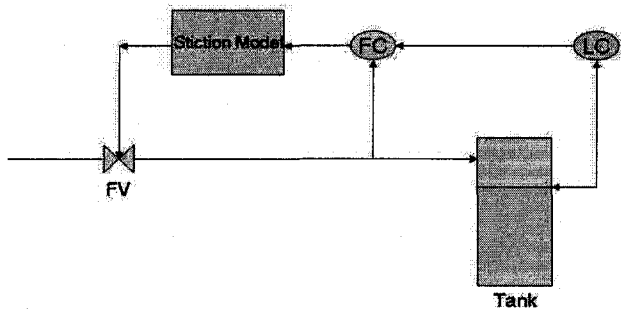

Figure 5.11: *Schematic of the cascaded level loop control*

Table 5.5: *Estimated S and J from experimental data*

	S		J	
Data	Actual	Estimated	Actual	Estimated
Flow Loop	1	1	1	1
	2	2	1	1.5
Level Loop	1	1	1	1
	2	1.5	1	0.5

5.6 Industrial Case Studies

This section summarizes the results of the proposed method on industrial data. For each loop, the set point (sp), controlled output (pv) and controller out- put (op) data were available. The numerical results for all loops are provided in Table 5.6. The proposed method is applicable to any type of control loops as shown in the Table.

Table 5.6: *Results for the Industrial Case studies*

		Estimated Stiction %	
Loop No.	Loop Type	S	J
1	Level	8	2
2	Flow	0.5	0.5
3	Temperature	1	1
4	Pressure	2	1
5	Composition	3	1

Loop 1 is the same level control loop described in section 5.1.1. The estimated S and J values are 8 and 2 respectively. This is verified using the valve positioner, mv (fortunately available in this case; but generally

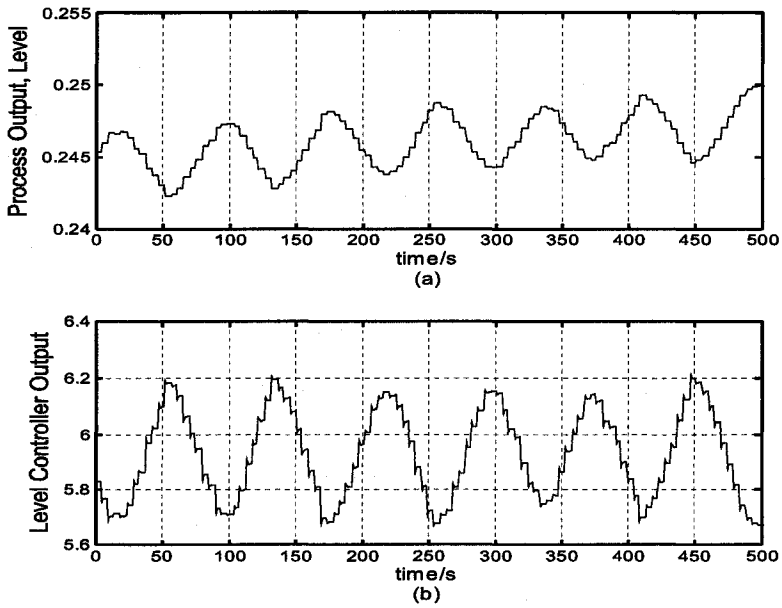

Figure 5.12: *(a) Process output (Level, PV) (b) Level controller output (OP)*

not available) and controller output, *op*. Figure 5.13 shows the (mv, op) for this case. The estimated J value matches well with the value seen in the plot. The S value is not exactly same but is close to the real value

Data for **loop 2** is obtained from a flow control loop of a refinery. The sampling interval for this data was 15 second. **Loop 3** is a temperature control loop on a furnace feed dryer system at Tech Cominco's mineral processing plant located in Trail, British Columbia, Canada. The temperature of the dryer combustion chamber is controlled by manipulating the flow rate of natural gas to the combustion chamber. For this loop, data were collected at a sampling interval of 1 min and over a period of two days leading to a total of 2880 samples. **Loop 4** data set had only 1500 data points collected at 20 s sampling intervals and corresponded to a pressure control loop in a refinery plant. **Loop 5** describes a concentration control loop. The data set contains 1100 data points collected at 1 s sampling intervals.

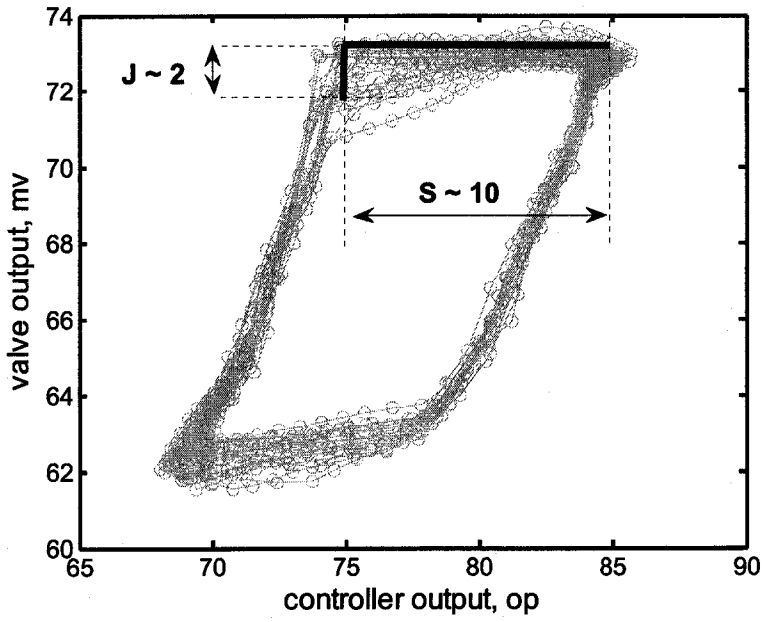

Figure 5.13: *mv-op plot for Industrial Level Loop (Loop 1).*

5.7 Summary

In this work, the effect of controller dynamics on the apparent stiction and the impact of J on the frequency and amplitude of limit cycles due to stiction have been demonstrated using simulation examples. A method is proposed to simultaneously estimate both S (stickband+deadband) and J (slip-jump). The stiction model parameters and the process model are jointly identified using an optimization approach. The proposed method has been tested successfully on simulated, experimental and industrial data. The method needs only routine operating data from a control loop.

6

Concluding Remarks and Future Directions

There has been extensive research done in the field of Process Monitoring and Assessment, in past decade and a half and various commercial process monitoring software tools are now available. Each toolbox has a different performance metric. In this work some practical issues related to Relative Performance Index (RPI) have been discussed. It has been shown through simulation examples that in presence of IWN type disturbance, RPI varies even if the controller tuning and the process model fidelity remain the same. A two step approach is taken to solve this problem:

1. Detect presence of IWN type disturbance in the system.
2. Calculate RPI for such cases.

A new index, Low Frequency Amplitude Ratio, $LFAR$ is developed which can be used to automatically detect the presence of IWN type disturbance in a system. The $LFAR$ value calculated for a system is compared to a critical $LFAR$ value, $LFAR_{critical}$. If $LFAR > LFAR_{critical}$ then the system is said to have IWN type disturbance. The $LFAR_{critical}$ value is user dependent. If the noise model is given by

$$N = \frac{1-\alpha}{1-\alpha q^{-1}} \tag{6.1}$$

then as $\alpha \rightarrow 0$, N→Integrator. But in real life pure integrators are rarely encountered. So, it is up to the user to decide for what value of 'α' will the system be considered to have IWN type disturbance. The $LFAR_{critical}$ and hence the final analysis is highly sensitive to this choice of 'α'.

It is demonstrated through simulation studies that for cases with IWN type disturbance, RPI computed based on the differenced data is relatively very stable. It is also shown that the differencing exercise does not mask the real change in the system (such as change in controller tunning).

RPI computation during set-point tracking is another issue with is dealt in this work. It has been shown through an industrial case study that the present way of computing RPI does not give accurate performance measure of a controller in a set-point tracking function. It is proved theoretically that the present way of computing RPI has some drawback when dealing with set-point tracking problems. A novel method is proposed to compute a performance metric for such cases. This method is based on fitting a BJ model to the process variable (pv) and then using step-response of the transfer function between process variable and the set-point to compute the performance metric. This metric is termed as RPI_{servo}. One possible problem with this technique is the issue of fitting a BJ model. This may be cumbersome in some cases.

Figure 6.1 is an extension of the logic flow diagram shown in chapter 1. The logic diagram shows the steps to calculate RPI. The logic is robust enough to handle the problem of varying RPI, (if the root-cause is the presence of IWN type disturbance in the system). It also provides an automatic technique to compute RPI for set-point tracking and regulatory control cases.

The economic impact analysis on better performance monitoring gives another dimension to the area of performance assessment and monitoring. In this work, an index, Economic Performance Index (EPI) has been developed. This index gives dual information, a measure of current controller performance and the economic benefits of improving the performance to a desired level. The concept of EPI is based on the variability reduction of the process output such that the operating point can be shifted closer to the constraint. This idea has been applied to an industrial case study and the results as evaluated by industrial personnel are considered credible.

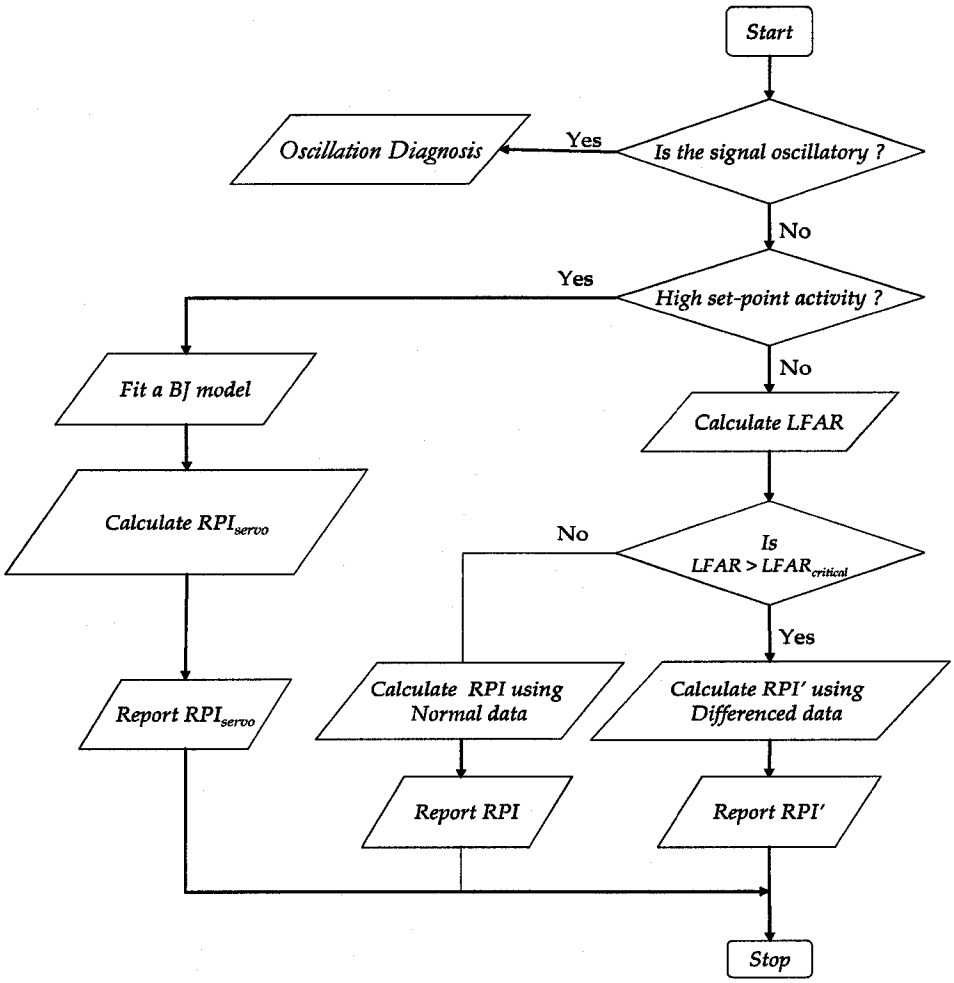

Figure 6.1: *Logic Flow Diagram to Compute appropriate RPI*

There are some issues / drawbacks with the present technique of evaluating EPI. The method to calculate the EPI does not take into account the loop interactions and variability transfer issues. In interacting loops, variance reduction in one process variable may effect the variance in the other loop. The method presented does not take this into account while computing the EPI. Another issue which is not considered in the present study is that variability reduction in the process output would mean increasing the variance of the manipulated variable. There may be constraints on the manipulated variable and in the method presented, these constraints are not taken into account.

A possible solution for this can be to first study the constraints on the manipulated variable(s) then taking them into account and work backwards to calculate the maximum allowed reduction in the variance of the process variable and then calculating the EPI accordingly. Also computing EPI in cases where the operating point cannot be changed, e.g. slave loop in a cascade system, still remains an open problem.

The last part of this work deals with quantification of stiction. The adequacy of two-parameter stiction model proposed by Choudhury *et al.* (2004*a*) over the one-parameter model, by Stenman *et al.* (2003) is established through an industrial example. The importance of slip-jump 'J' is also established through a simulation example.

A novel method to quantify stiction using a two-parameter model has been proposed. The method has been successfully tested on simulated, experimental and industrial data sets. The method is based on the identification of a hammerstein model. Therefore, in cases with no stiction present, the problem of persistent excited input signal comes in and the results can not be trusted. Therefore the first step before implementing this technique is to detect stiction using the stiction detection methods available in literature.

The stiction model used in this method in its slightly modified form can also handle asymmetric stiction. Therefore it is possible to extend the method to estimate parameters of asymmetric stiction model. The proposed method can also be extended to cases when the plant model is nonlinear in itself. In such cases, to correctly estimate S and J, knowledge of the presence and structure of the non-linearity is required.

The proposed method is found to be sensitive to the data set chosen for quantification, i.e. if data set is not chosen carefully, then the proposed technique may give misleading results. A method is needed to automatically select the best representative data set from the available data.

Bibliography

Bauer, Margret and Ian K Craig (2006). Economic performance assessment of apc projects - a review and framework. In: *Proceedings of SICOP*.

Bialkowski, W. L. (1993). Dreams vs. reality: A view from both sides of the gap. *Pulp and Paper Canada*.

Choudhury, M. A. A. S., N. F. Thornhill and S. L. Shah (2004*a*). Modelling valve stiction. *Control Engng. Prac., In press*.

Choudhury, M. A. A. S., S. L. Shah and N. F. Thornhill (2002). Detection and diagnosis of system nonlinearities using higher order statistics. In: *15th IFAC World Congress*. Barcelona, Spain.

Choudhury, M. A. A. S., S. L. Shah and N. F. Thornhill (2004*b*). Detection and quantification of control valve stiction. In: *The proceedings of DYCOPS 2004, July 5-7, 2004*. Cambridge, USA.

Choudhury, M. A. A. S., S. L. Shah and N. F. Thornhill (2004*c*). Diagnosis of poor control loop performance using higher order statistics. *Automatica* **40**, 1719–1728.

Choudhury, M. A. A. S., S. L. Shah, N. F. Thornhill and D. S. Shook (2005). An automatic method for detection and quantification of stiction in control valves. *Control Engng. Prac., to appear*.

Desborough, L. and T. J. Harris (1993). Performance assessment measures for univariate feedforward / feedback control. *The Canadian Journal of Chemical Engineering*.

Ender, D. (1993). Process control performance: Not as good as you think. *Control Engineering* **40**, 180–190.

Eriksson, P. G. and A. J. Isaksson (1994). Some aspects of control loop performance monitoring. In: *Proceedings of the Third IEEE Conference on Control Applications*. Vol. 2. Glasgow, Scotland. pp. 1029 – 1034.

Gao, J., R. Patwardhan, K. Akamatsu, Y. Hashimoto, G. Emoto, S. L. Shah and B. Huang (2003). Performance evaluation of two industrial mpc controllers. *Control Engineering Practice* **11**, 1371–1387.

Harris, T., F. Boudreau and J. F. MacGregor (1996). Performance assessment of multivariable feedback controllers. *Automatica* **32**, 1505 – 1518.

Harris, T. J. (1989). Assessment of control loop performance. *The Canadian Journal of Chemical Engineering*.

Horch, A. (1999). A simple method for detection of stiction in control valves. *Control Engng. Prac.* **7**, 1221–1231.

Horch, A. and A. J. Isaksson (1998). A method for detection of stiction in control valves. In: *Proceedings of the IFAC workshop on On line Fault Detection and Supervision in the Chemical Process Industry*. Lyon, France.

Huang, B. and S. L. Shah (1998). Practical issues in multivariable feedback control performance assessment. *Journal of Process Control* **8**, 421 – 430.

Huang, B. and S. L. Shah (1999). *Performance Assessment of Control Loops*. Springer-Verlag London Ltd. London UK.

Huang, B., S. L. Shah and E. K. Kwok (1997). Good, bad or optimal? performance assessment of multivariable processes. *Automatica* **33**, 1175 – 1183.

Huang, B., S. L. Shah and R. Miller (2000). Feedforward plus feedback controller performance assessment of mimo systems.. *IEEE Transactions on Control Systems Technology* **8**, 580 – 587.

Hugo, A. J. (2006). Performance assessment of industrial controllers. In: *Proceedings of Chemical Process Control 7*. Lake Louise, Canada.

Jelali, M. (2006). An overview of control performance assessment technology and industrial applications. *Control Engineering Practice* **14**, 441 – 466.

Ko, B. S. and T.F. Edgar (2001). Performance assessment of multivariable feedback control systems. *Automatica* **37**, 899 – 905.

Lynch, C. and G. A. Dumont (1996). Control loop performance monitoring. *IEEE Transactions on Control Systems Technology* **18**, 151 – 192.

McNabb, C. A. and S. J. Qin (2003). Projection based mimo control performance monitoring: i - covariance monitoring in state-space. *Journal of Process Control* **13**, 739 – 757.

McNabb, C. A. and S. J. Qin (2005). Projection based mimo control performance monitoring: ii - measured disturbances and setpoint changes. *Journal of Process Control* **15**, 89 – 102.

Muske, K. R. (2003). Estimating the economic benefits from improved process control. *Ind. Eng. Chem. Res.* **42**, 4535–4544.

Rinchart, N. and F. Jury (1997). How control valves impact process optimization. *Hydrocarbon Processing*.

Singhal, A. and T. I. Salsbury (2005). A simple method for detecting valve stiction in oscillating control loops. *Journal of Process Control* **15**, 371.

Srinivasan, R., R. Rengaswamy and R. Miller (2005*a*). Control loop performance assessment:i. a qualitative approach for stiction diagnosis. *Ind. Eng. Chem. Res.* **44**, 6708–66718.

Srinivasan, R., R. Rengaswamy, S. Narasimhan and R. Miller (2005*b*). Control loop performance assessment:ii. hammerstein model approach for stiction diagnosis. *Ind. Eng. Chem. Res.* **44**, 6719–66728.

Stanfelj, N., T. E. Marlin and J. F. MacGregor (1993). Monitoring and diagnosing process control performance: The single-loop case. *Ind. Eng. Chem. Res.* **32**, 301–314.

Stenman, A., F. Gustafsson and K. Forsman (2003). A segmentation-based method for detection of stiction in control valves. *Int. J. Adapt. Control Signal Process.* **17**, 625–634.

Swanda, A. P. and D. E. Seborg (1999). Controller performance assessment based on setpoint response data. In: *Proceedings of the American Control Conference*. Vol. 6. San Diego, California. pp. 3863 – 3867.

Taha, O., G. A. Dumont and M. S. Davies (1996). Detection and diagnosis of oscillations in control loops. In: *Proceedings of* 35^{th} *conference on Decision and Control*. Kobe, Japan.

Thornhill, N. F., B. Huang and S. L. Shah (2003). Controller performance assessment in set point tracking and regulatory control. *International Journal of Adaptive Control and Signal Processing* **17**, 709 – 727.

Tyler, M. and M. Morari (1995). Performance assessment for unstable and nonminimum-phase systems. In: *Preprints IFAC workshop on-line fault detection supervision chemical process industries*. Newcastle, UK.

Tyler, M. and M. Morari (1996). Performance monitoring of control systems using likelihood methods.. *Automatica* **32**, 1145 – 1162.

Wallén, A. (1997). Valve diagnostics and automatic tuning. In: *Proceedings of American Control Conference*. Albuquerque, New Mexico. pp. 2930–2934.